COLUMN HYDRODYNAMICS OF SOLVENT IN PULP PROCESSING

by

DAVID W. KOREN

Ottawa, Ontario, 1986

A thesis
presented to the University of Ottawa
in fulfillment of the
thesis requirement for the degree of
MASTER OF APPLIED SCIENCE
in
CHEMICAL ENGINEERING

ISBN 0-315-36502-1

UNIVERSITÉ D'OTTAWA
UNIVERSITY OF OTTAWA

ABSTRACT

The hydrodynamics of solvent-in-pulp processes have been studied by determining the effects of the addition of solids to the aqueous phase of a 10.76 cm I.D. pulsed column. Dispersed phase hold-up and drop sizes were measured in order to identify these effects.

In order to evaluate the relationships between hold-up and the operating variables a factorial design was carried out. The variables studied were the pulse frequency and the aqueous and organic flow rates. It was found that a modified polynomial model fit the experimental data adequately.

Initial tests carried with a solids-free feed determined the effects of plate free area and amplitude on the hold-up. With the addition of solids, hold-up decreased while drop size increased over the entire experimental range. These results are explained by considering drop mechanics as well as the surface phenomena that exist at the interface.

Tests carried out to determine the influence of particle size showed that, although there was no apparent change in hold-up, solvent entrainment increased. The aqueous phase pH, although changing the surface properties of the sand, was not found to significantly affect the hold-up.

ACKNOWLEDGEMENTS

I wish to express my gratitude to Dr. J.A. Golding for guidance and encouragement throughout this work. I am also very grateful to Elaine Koren without whom this work would not have been possible.

Thanks also go to J. Gasparetti, A. Bonaldo and D. Lefebvre for their technical assistance through the course of this work. Dr. Soles from Energy, Mines and Resources (E.M.R.) is also acknowledged for his help with the Zeiss particle size analyser. Also to E.M.R. for providing the organic phase that was used.

Finally, I wish to thank the Natural Sciences and Engineering Research Council of Canada from whom financial support was provided.

NOMENCLATURE

Symbols in the text, unless otherwise stated, have the following meaning:

a	specific interfacial area (cm^2/cm^3)
A	pulse amplitude (cm)
B_i	parameters in proposed model
C_i	constants
C_D	drag coefficient
d	orifice diameter (cm)
D	drop diameter (cm)
D_e	equivalent drop diameter (cm)
D_N	nozzle diameter (cm)
D_{min}	minimum diameter (cm)
D_{max}	maximum diameter (cm)
D_{32}	Sauter mean diameter (cm)
e	residual
E	energy dissipation (m^2/sec^3)
F	pulse frequency (min^{-1})
F_b	buoyant force (N)
F_s	interfacial tension force (N)
g	gravitational constant (9.80 m/sec^2)
K	constant introduced by Khemangkorn
n	total number of data points

N	axial height (m)
p	number of parameters
Q	volumetric flow rate (ml/min)
r_a	reaction rate per unit area (mol/sec m^2)
r'_a	total reaction rate (mol/sec)
s^2	sample variance
V	volume of dispersion (m^3)
V_c	continuous phase superficial velocity (cm/min)
V_d	dispersed phase superficial velocity (cm/min)
V_{FS}	liquid drop volume (m^3)
$\bar{V}_o$	mean characteristic velocity (m/sec)
V_{slip}	drop velocity relative to continuous phase (m/sec)
V_t	terminal drop velocity (m/sec)
X_1	coded pulse frequency
X_2	coded aqueous flow rate
X_3	coded organic flow rate
X_d	dispersed phase hold-up

Greek symbols:

α	plate free area
β	$\alpha/(1-\alpha)(1-\alpha^2)$
ψ	parameter introduced by Miyauchi and Oya
ψ_{mod}	parameter introduced by Kumar and Hartland
μ_c	viscosity of the continuous phase (Pa.sec)
μ_d	viscosity of the dispersed phase (Pa.sec)
ν	degrees of freedom related to a measurement

ρ_c	density of the continuous phase (kg/m^3)
$\Delta\rho$	density difference (kg/m^3)
ℓ	axial distance between plates (m)
θ	contact angle
σ	interfacial tension (mN/m)

CONTENTS

FIGURES

TABLES

Chapter I

INTRODUCTION

Although pulsed sieve plate extraction columns are now used in the minerals industry, only clarified solutions are being processed. Since small amounts of fine solids cause crud problems, an extensive series of processing steps are carried out to prepare these solutions. However, if a pulsed column could treat dilute slurry systems the need for filtration would be eliminated while application to heavy slurries would make both sand-slime and filtration steps unnecessary. This would be very advantageous since the costs of these latter operations account for a considerable portion of the processing cost. In addition, as lower grades are being processed, incentives exist to eliminate preliminary operations. For example, in the uranium industry, solid-liquid purification steps represent the second largest capital cost (30%) and from 10-20% of the operating cost [1]. Although this problem has been recognized, little work has been done in this field [2-5]. Ritcey et al [3], provided a comparison of processing costs for clarified and non-clarified solutions. The costs are shown in Table 1 and indicate there is potential for a considerable saving by processing slurry feeds. Solvent extraction of slurries is

complicated by losses of solvent due to adsorption on the solids. This loss can make many such separations unprofitable.

Table 1: COMPARISON OF COSTS OF SOLVENT EXTRACTION

Elliot Lake Ore is being treated at a rate of 3000 tons per day and a concentration of 0.1% Uranium (U). The costs are cents per pound of U.

PROCESSING STEP	CLARIFIED SOLUTION	UNCLARIFIED SOLUTION
Liquid-solid Separation		
Operating	13	--
Equipment	14	--
Solvent Filtration	--	0.5
Solvent Loss	8.3	12.5
Elution or Stripping Reagents	1.2	1.2
Depreciation of Solvent Inventory	0.4	0.4
Depreciation of Equipment	3.3	5.6
Labour and Maintenance	2.5	3.0
TOTAL	42.7	23.2

Note: Unclarified Solution consists of a 35% solids slurry of size range 40% -200 mesh.

Before this process is to be accepted by industry, knowledge concerning hydrodynamics and operating regions must be obtained. The work carried out in this study provides the initial stages in the development of such principles. It was

undertaken to provide fundamental data on the hydrodynamics of pulsed column operation. To obtain this, the flow rates and pulse frequency were varied while the dispersed phase hold-up and drop sizes were measured. The results also help to provide insight into other factors that govern this three phase system.

Chapter II

LITERATURE SURVEY

2.1 PULSE COLUMN DESCRIPTION

2.1.1 OPERATING CHARACTERISTICS

The pulse column was patented by Van Dijk [6] in 1935. He proposed that the efficiency of a column extractor could be greatly increased by the application of an oscillating pulse to the contents of a column. This was shown to increase both turbulence and interfacial area. A schematic of a pulsed sieve plate column is given in Figure 1.

Both liquids are fed continuously into the column flowing countercurrently along the column and are withdrawn from opposite ends of the column. When the holes in the plates are small and the interfacial tension between the phases large no flow will occur in the column unless a pulsing action is introduced. When this additional up and down movement is added, the two liquids are alternately forced through the plates. In this manner, a vertical pumping action is imposed on the countercurrent flow of the two phases, dispersing one of the phases (dispersed phase) as it is forced through the holes and mixing the other (continuous phase). It is possible to disperse either the light or heavy phase depending on the operating preference.

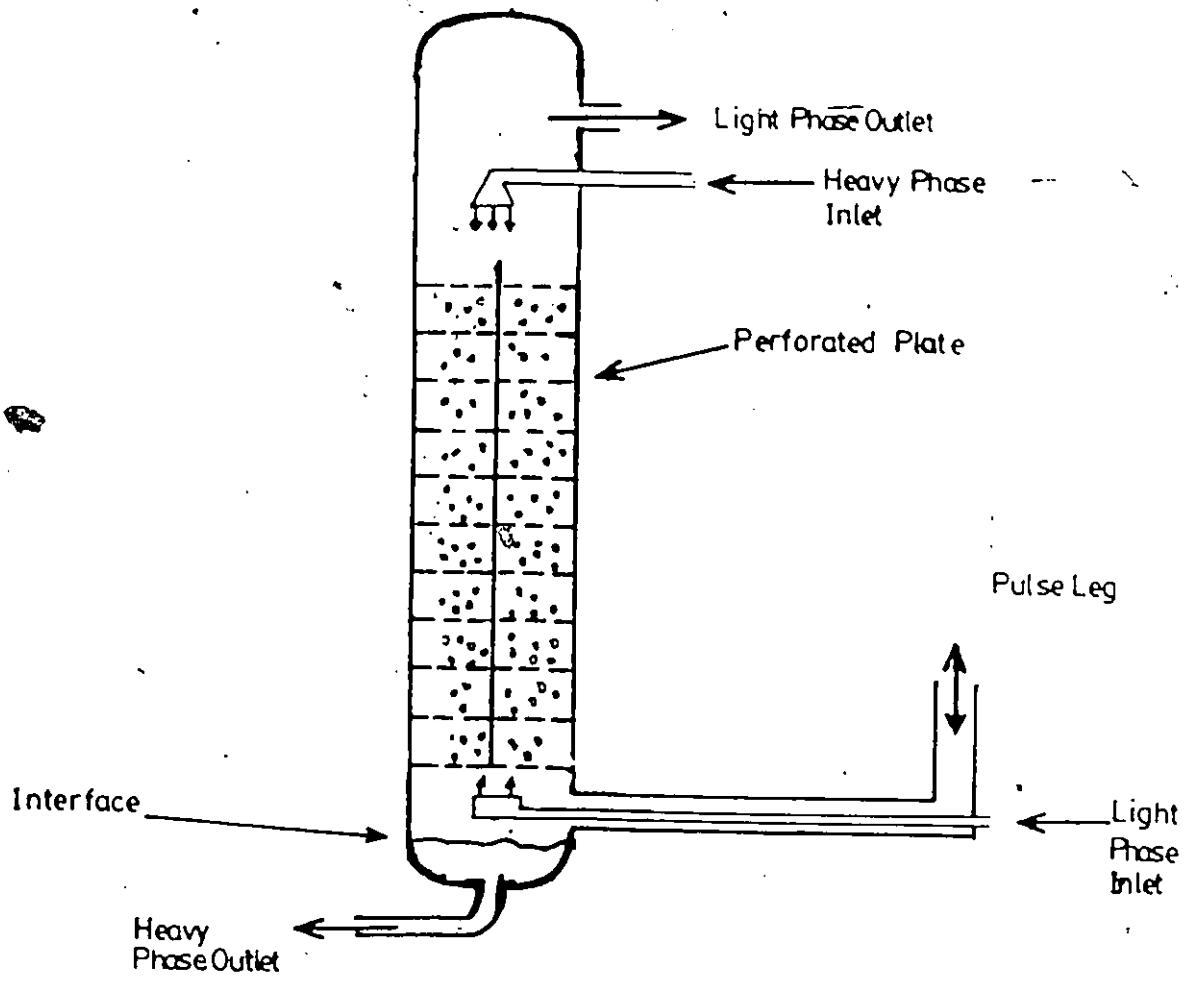

FIGURE 1: PULSED COLUMN

The operating characteristics of the column are usually represented on a plot of total flow (i.e. flow of continuous phase + flow of dispersed phase) versus pulsation intensity (i.e. frequency of pulse × amplitude of pulse) after Sege and Woodfield [7]. Two general regions are recognized, flooding and non-flooding (see Figure 2). In pulsed operation flooding is defined as occurring when a phase is discharged from the end of the column by which it enters. The non-flooding or operating region can further be divided as illustrated in Figure 3.

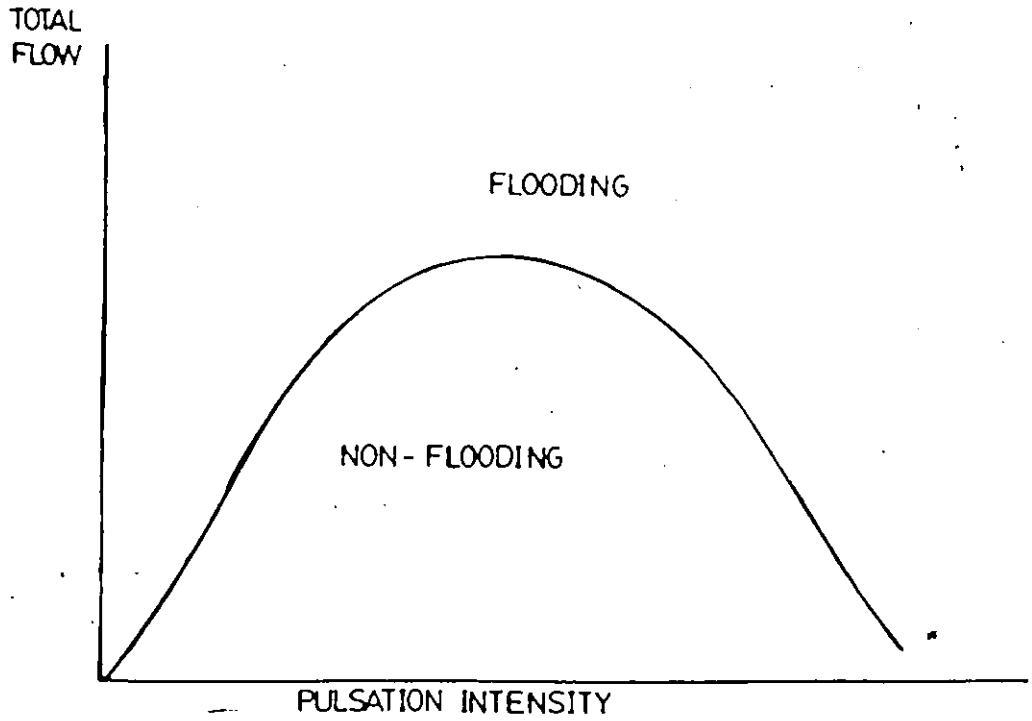

FIGURE 2: FLOW REGIMES OF A PULSED COLUMN

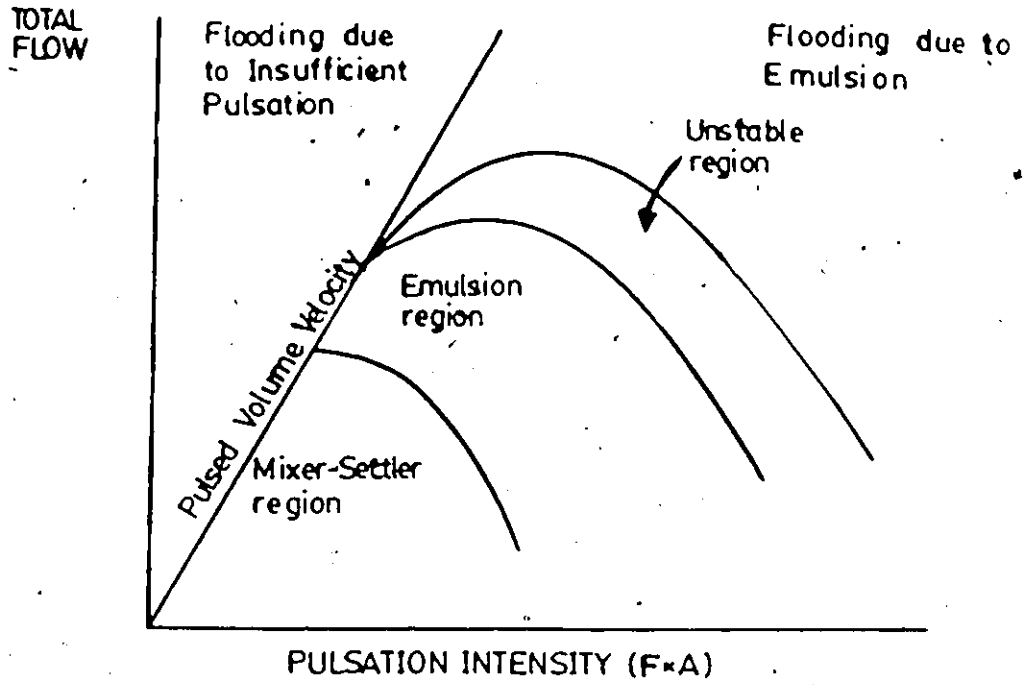

FIGURE 3: OPERATING REGIONS

At low pulse intensities and flow rates, the discontinuous phase alternately disperses and coalesces in the space between the plates (see Figure 4a). This type of operation is termed 'mixer-settler' since the two phases behave as they would in a mixer-settler contactor. In this region, if the phases are fed into the column at a rate faster than they can be pumped through the column by the pulsing action they will build-up in volume in their respective inlet zones. Eventually, this accumulation will approach that of the outlet zone and they will be forced through the outlet

of the opposite phase. This type of flooding is referred to as 'flooding due to insufficient pulsation'. It has been proposed [7] that this type of flooding will occur unless the pulsed volume at least equals the volumetric rate of flow, or

$$V_d + V_c \leq (A \times F) \qquad (1)$$

As the pulsing action is increased (i.e. increase frequency and/or amplitude of the pulse) the inertial and shear forces also increase. Due to this, dispersed phase coalescence between pulse strokes is reduced and eventually a uniform dispersion is formed (see Figure 4b). This manner of operation provides the best mass transfer rates [8] as a result of the large surface area and good mixing that is present. This region is referred to as the 'emulsion' region. In this zone, the more vigorous the pulsing, the finer is the resulting emulsion. A transition zone preceeding the emulsion zone on the operating diagram was proposed by Hafez et al [9], and was termed the 'dispersion' region. It was introduced because it was found that both hold-up and flooding velocity correlations display distinct features in this region. At higher pulse intensities, a further region is recognized, it is referred to as the 'unstable' region. Here, the emulsion becomes unstable and coalescence and phase inversion occurs (see Figure 4c). Evident from this discussion is the effect pulsing conditions and the operat-

ing region have on the properties of the emulsion. The manner in which some of these properties vary will now be described.

(A) MIXER-SETTLER REGION

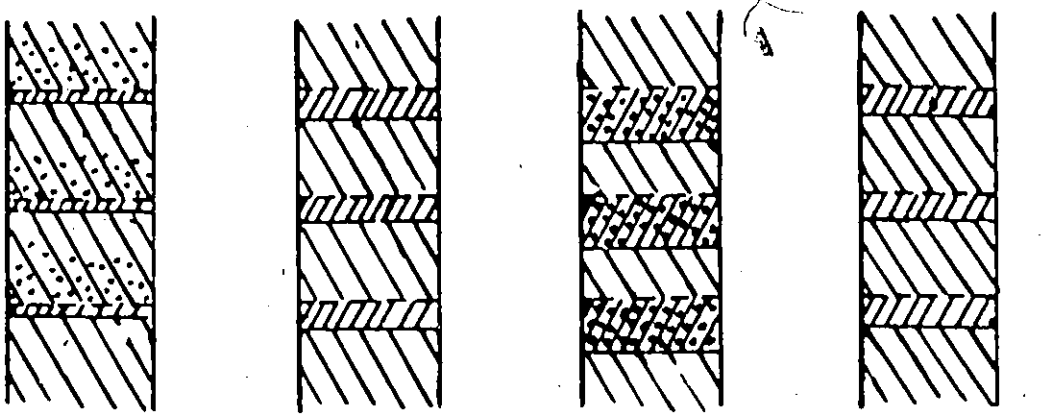

(B) EMULSION REGION

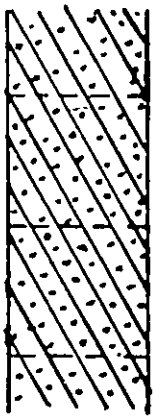

(C) UNSTABLE REGION

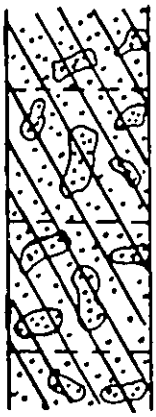

FIGURE 4: QUALITATIVE MEANS OF DISTINGUISHING REGIONS OF OPERATION.

2.1.2 DISPERSED PHASE HOLD-UP

One of the most important properties of the emulsion is the total volume of the dispersed phase between the plates. The hold-up, as it is also known, determines column throughput and together with drop size determines interfacial area available for mass transfer. It is generally reported as the average value of hold-up over the entire column although there is evidence that it varies along the column length [16,31,32]. A measurement is obtained by shutting the dispersed inlet after reaching equilibrium and recording the change in the interface level after the phases have settled. Other methods of obtaining hold-up measurements are also in use. Cermak [33] describes a method that involves the determination of the liquid density, while Jiricny and Prochazka [31] use a method of differential pressure measurements.

As reported by Sehmel and Babb [10], the hold-up decreases with increasing pulse intensity (i.e. F×A) in the mixer-settler region. In this case, the dispersed phase gets pumped through the column at an increased rate by the pulsing action, thus the residence time and consequently the hold-up decreases. The disappearance of the dispersed phase layer and the appearance of a uniform distribution of the dispersed phase in the form of drops is indicative of transfer to the emulsion region, the boundary between the two is usually recognized as occurring at the the minimum hold-up.

The frequency at this minimum is referred to as the transition frequency. In the emulsion region, as the frequency or amplitude increases, the droplet population decreases because the smaller drops produced fall or rise at a lower velocity, therefore their residence time between the plates is greater. In this zone, the hold-up increases with increasing pulsing conditions. The hold-up becomes maximum at the transition between the 'emulsion' and the 'unstable' regions [10]. The behaviour generally observed is illustrated in Figure 5.

Due to the importance of the hold-up in the design of the column, a number of correlations have been proposed. The complexity of the operation has led many to take an empirical approach. One of the earliest attempts was made by Logsdail and Thornton [34] in 1957. They proposed correlating flow rates and the dispersed phase hold-up (X_d) by:

$$\frac{V_d}{X_d} + \frac{V_c}{(1-X_d)} = \bar{V}_o(1-X_d) = V_{slip} \qquad (2)$$

Here $\bar{V}_o$ is the mean droplet velocity relative to the continuous phase when $V_c=0$ and $V_d \to 0$ [11]. Using the expression above, the hold-up can be predicted provided a suitable correlation for $\bar{V}_o$ is available. Some have been proposed by Niebuhr and Vogelpohl [13], Batey et al [11] and Thornton [12]. The relationship in Equation (2) has been shown to be

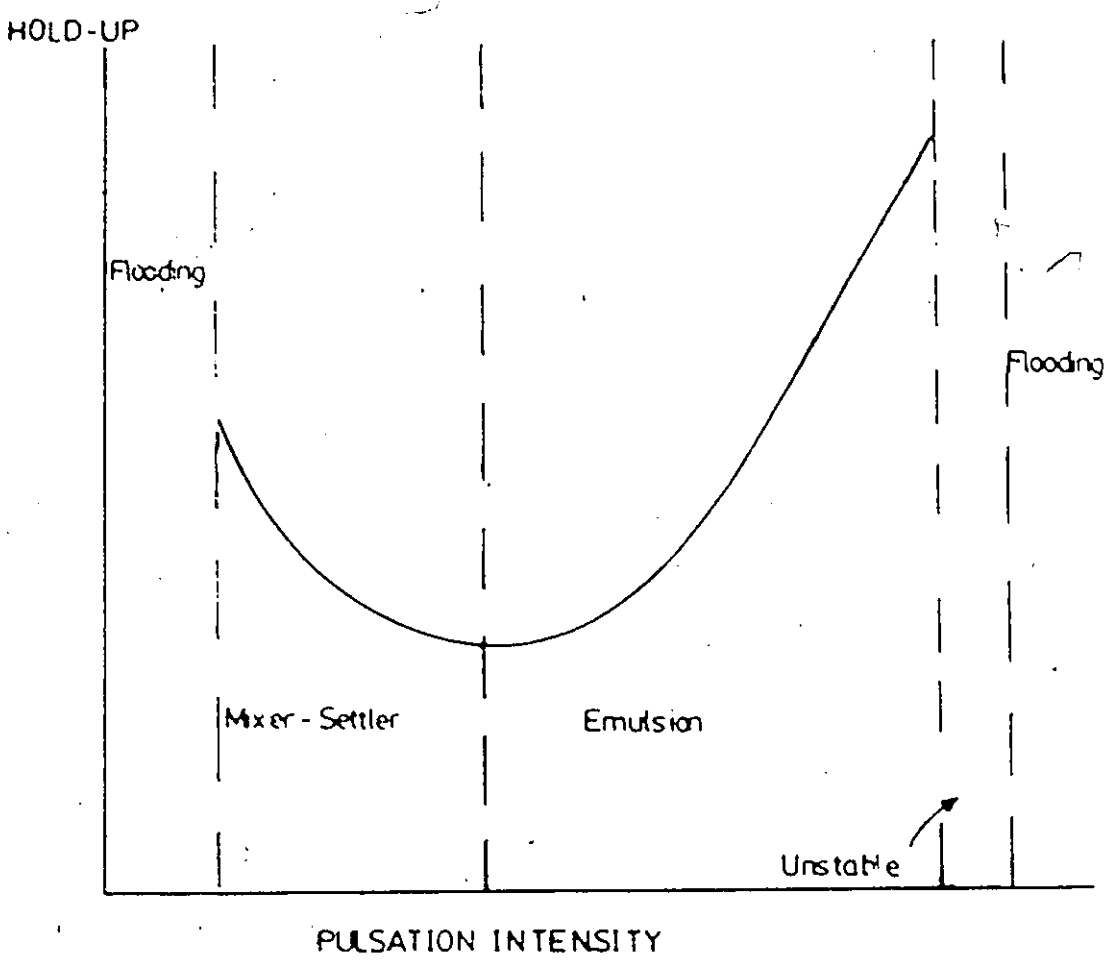

FIGURE 5: RELATIONSHIP BETWEEN HOLD-UP AND PULSATION INTENSITY

valid only when drop coalescence is absent (i.e.in the emulsion region). Sato et al [39] proposed correlations for each of the operating regions:

Mixer-settler region

$$X_d = 0.52\left(\frac{A\times F}{V_d}\right)^{-0.70}\left(1+\frac{V_d}{V_c}\right)^{-0.70}\ell^{-1.2}d^{-0.26}$$

$$\text{for } 0 \leq A\times F \leq 1.3V_d^{0.22}\ell^{-0.32}d^{-0.37} \qquad (3)$$

Dispersion region

$$X_d = 0.42(A\times F)V_d^{0.33}\left(1+\frac{V_d}{V_c}\right)^{-0.70}\ell^{-0.68}d^{0.37}$$

$$\text{for } 1.3V_d^{0.22}\ell^{-0.32}d^{-0.37} \leq A\times F \leq 0.8V_d^{0.22}\ell^{0.35}d^{-0.37} \qquad (4)$$

Emulsion region

$$X_d = 0.54(A\times F)^{2.4}\left(1+\frac{V_d}{V_c}\right)^{-0.70}\ell^{-1.2}d^{0.89}$$

$$\text{for } A\times F \geq 0.8V_d^{0.22}\ell^{0.35}d^{-0.37} \qquad (5)$$

Miyauchi and Oya [14] later introduced the mean rate of energy dissipation and proposed a criterion by which the hydrodynamic operating region can be assessed. This was based on values of the parameter ψ, as defined below:

$$\psi = \frac{A\times F}{(\beta\ell)^{1/3}}\left(\frac{\mu_d^2}{\sigma\Delta\rho}\right)^{1/4} \qquad (6)$$

where β is a function of the plate free area, α. In a plot of hold-up versus ψ a marked change in slope was observed at ψ=0.21, which marked the transition between mixer-settler and emulsion operation. On this basis, correlations for each region were provided as:

$$X_d = 0.66 V_d^{2/3} \psi^{0.84} \quad \text{for } \psi < 0.21 \tag{7}$$

$$X_d = 6.32 V_d^{2/3} \psi^{2.4} \quad \text{for } \psi > 0.21 \tag{8}$$

Arthayukti [40] obtained a similiar relationship in which pulse intensity was used to assess the operating region:

$$X_d = 0.38 V_d^{2/3} \psi^{0.75} \quad \text{for } A\times F < 4.57 \text{ cm/sec} \tag{9}$$

$$X_d = 3.46 V_d^{2/3} \psi^{2.62} \quad \text{for } A\times F > 4.57 \text{ cm/sec} \tag{10}$$

Modifications in these relationships were provided by Kumar and Hartland [15]. The parameter ψ was made dimensionless and a new intermediate correlation was provided to account for a transition region between those suggested by Miyachi and Oya. From Kumar and Hartland [15]:

$$\psi_{mod} = \frac{(A\times F)^3}{\beta \ell} \frac{\rho_c}{\Delta\rho^{3/4} \sigma^{1/4} g^{5/4}} \tag{11}$$

for the dispersion region (i.e. $\psi_{mod}<0.05$):

$$X_d = 6.91\left[\frac{(A\times F)^3\rho_c^{1/4}}{\beta\ell\sigma^{1.4}g^{5.4}}\right]^{0.31}\left[\frac{V_d^4\rho_c}{g\sigma}\right]^{0.30} \times\left[1+\frac{V_c}{V_d}\right]^{0.14}\left[\frac{\Delta\rho}{\rho_c}\right]^{-0.79}\left[\frac{\mu_d^4 g}{\rho_c\sigma^3}\right]^{-0.01} \quad (12)$$

for the emulsion region (i.e. $\psi_{mod}>0.05$):

$$X_d = 3.73\times10^{-3}\left[\frac{(A\times F)^4\rho_c}{g\sigma}\right]^{0.62}\left[\frac{V_d^4\rho_c}{g\sigma}\right]^{0.31} \times\left[1+\frac{V_c}{V_d}\right]^{0.45}\left[\frac{\Delta\rho}{\rho_c}\right]^{-2.20}\left[\frac{\mu_d^4 g}{\rho_c\sigma^3}\right]^{-0.29} \quad (13)$$

for the mixer-settler region (i.e. $\psi_{mod}<0.05$):

$$X_d = 3.91\times10^{-3}\left[\frac{A^2\rho_c g}{\sigma}\right]^{-0.26}\left[\frac{F^4\sigma}{\rho_c g^3}\right]^{-0.19} \times\left[\frac{V_d^4\rho_c}{g\sigma}\right]^{0.28}\left[1+\frac{V_c}{V_d}\right]^{0.19} \times\left[\frac{\Delta\rho}{\rho_c}\right]^{-0.81}\left[\frac{\mu_d^4 g}{\rho_c\sigma^3}\right]^{-0.19} \quad (14)$$

The model proposed by Bell and Babb [16] enables the hold-up to be calculated in all three regions of pulsed sieve plate column operation, and is shown below:

$$X_d = V_d\{C_1+(C_2+C_3V_c)(AF-C_4)^2\} \quad (15)$$

It requires the empirical determination of the constants C_1 and C_4, which depend on the physical properties of the liquid-liquid system and C_2 and C_3, which depend on the column geometry [15].

2.1.3 INTERFACIAL AREA

Another important property of the emulsion is the specific interfacial area. Liquid-liquid extraction processes demand the transfer of a solute between an aqueous and organic phase, the rate of this transfer will be directly proportional to the surface area present. The area available for mass transfer per unit volume can be obtained if the hold-up and an estimate of the drop size is known. If the drops are spheres it can be shown that:

$$a = \frac{6 \times X_d}{D_{32}} \tag{16}$$

For spheres, the Sauter Mean Diameter, D_{32}, can be estimated from drop diameters as observed from a photograph of the emulsion, according to the following:

$$D_{32} = \frac{\Sigma D_i^3}{\Sigma D_i^2} \tag{17}$$

For non-spherical drops, the major and minor axes of the drops are measured and used to calculate an equivalent diameter according to the following:

$$D_c = (D_{min} D_{max}^2)^{1/3} \tag{18}$$

Khemangkorn et al [17] proposed that at equilibrium, D_{32} will be a function of energy dissipation and the physical properties of the liquids as given by:

$$D_{32} = K\left(\frac{\sigma}{\rho_c}\right)^{0.60} E^{-0.40} \tag{19}$$

For a given column construction, it can be shown that Equation (19) reduces to:

$$D_{32} = K'\left(\frac{\sigma}{\rho_c}\right)^{0.60} (A \times F)^{-1.20} \tag{20}$$

Although the above relationship provides a starting point it has been shown [17] that an expression of the form:

$$D_{32} = C_1 \, A^{C_2} \, F^{C_3} \, N^{C_4} \tag{21}$$

fits data better. To account for system properties, Equation (21) is modified to include the term $(\sigma/\Delta\rho g)$. In his final model, Khemangkorn et al [17] also included the superficial velocity of the dispersed phase.

Correlations reported in the literature do not generally differentiate between operating regions, but those presented here are assumed to be valid for high agitation rates

(i.e.in the emulsion region). For mild agitation, the equation

$$D_{32} = \left(\frac{\sigma}{g\Delta\rho}\right)^{0.50} \tag{22}$$

can be used to indicate a maximum drop diameter [34].

Another method of determining surface area is described by Nanda and Sharma [35]. In this method, liquid extraction is accompanied by fast pseudo first-order reaction to evaluate the area directly. The total reaction rate r_a estimated experimentally and the theoretical value r'_a are used as follows:

$$a = \frac{r'_a}{r_a V} \tag{23}$$

to obtain the effective interfacial area. When using this method Fernandes [36] reported results similiar to those obtained using indirect means.

2.2 SOLVENT IN PULP PROCESSING

The majority of research in solvent-in-pulp (S.I.P) processing has been concerned with uranium recovery [2-5]. Initial work carried out with mixer-settlers by Ellis et al [18] and Grinstead et al [19] proved to be unsuccessful because the high agitation used caused stable emulsions and crud formation which gave rise to large solvent losses. For example,

in the treatment of 50 wt. percent slurries with 0.1 M monododecyl phosphoric acid in kerosene, Ellis et al found that entrainment varied from 7-15 gallons of organic per ton of solid. It was found that these losses could be reduced substantially by maintaining the organic phase as the continuous phase and with a high organic to aqueous ratio (e.g. 750). Similiar results were reported by North and Wells [20] using a rotary film contactor. It was further noted that using tertiary amines stable emulsions were formed and half of the amine was adsorbed on the solid surface. These results made solvent-in-pulp processing uneconomic.

Burger and Jardine [21] showed however that a slurry of 10 weight percent solids could be treated in a pulsed column. Subsequent work at Eldorado Nuclear [5] established that economically successful operations could be carried out by careful control of the pulsing conditions. Joe et al [5] reported that when using slurries, flow rates and pulsing conditions should be cut in half to prevent emulsion formation. Under these conditions a 30-40 wt. percent solids containing 90% -200 mesh (75μm) could be treated so that the amine loss was down to an economically acceptable level of 0.015 gallons amine per ton of dry feed. Energy, Mines and Resources (E.M.R.) in Ottawa carried out more extensive studies with a similiar system. Tests with both aqueous and organic continuous systems were performed. Ritcey et al [3] reported that, physically, organic continuous operation is

superior and provides the best potential for reducing solvent losses. Further studies with this type of operation were not carried out. For aqueous continuous operation, Ritcey et al recommended the following to reduce solvent losses:

1. sieve plates made of stainless steel rather than teflon
2. plates with holes of 3/16 inch diameter instead of those of 1/8 inch
3. decrease pH from 2.7 to 1.35
4. decrease frequency of pulse from 60 to 35 cycles/min
5. decrease plate spacing from 4 to 2 inches
6. wash or wet the solids with kerosene prior to extraction

In the studies outlined, extraction usually presented no problem with a slurry system. The high losses of solvent, though, prompted many workers to study this problem further. Ellis et al [18] found that the addition of hydrophilic surfactants of the organic sulfonate type reduced entrainment losses. Tolun [22] showed that by changing the pH of a system containing tri-iso-octyl amine (extractant) solvent losses are affected due to the formation of a surfactant. Wilkinson [23] also noted that surface properties of the solids present play a role in stable emulsion formation and thus solvent losses. As pointed out by Tolun [22], these systems resemble in many ways those encountered in flotation

operations. Hydrophobic collecting agents that are preferentially adsorbed at the organic-solid interface will collect the solid particles at the interface and stabilize the emulsion. Dispersing agents which make the particles hydrophilic would act in the opposite manner. By performing studies similiar to those usually carried out on flotation systems, losses could be reduced.

Chapter III

THEORETICAL CONSIDERATIONS

The factors influencing hold-up and drop size in normal pulsed column operation can also be expected to affect these properties in solvent-in-pulp processing. However, as a third phase is added, surface phenomena must also be considered as well as droplet formation. The basic principles involved are discussed in the following sections.

3.1 DROP MECHANICS

Drops are formed in sieve plate column extractors by dispersing one of the liquid phases into the other through a series of orifices. There are four major forces acting on a drop during the process of formation at an orifice. The buoyancy force due to the difference in densities between the two phases and the inertial or kinetic force associated with the fluid flowing out of the nozzle act to separate the drop from the nozzle, while the interfacial tension force at the nozzle tip and the drag force exerted by the continuous phase act to keep the drop on the nozzle [24]. When the lifting force exceeds the restraining force, the drop begins to break away from the nozzle (see Figure 6).

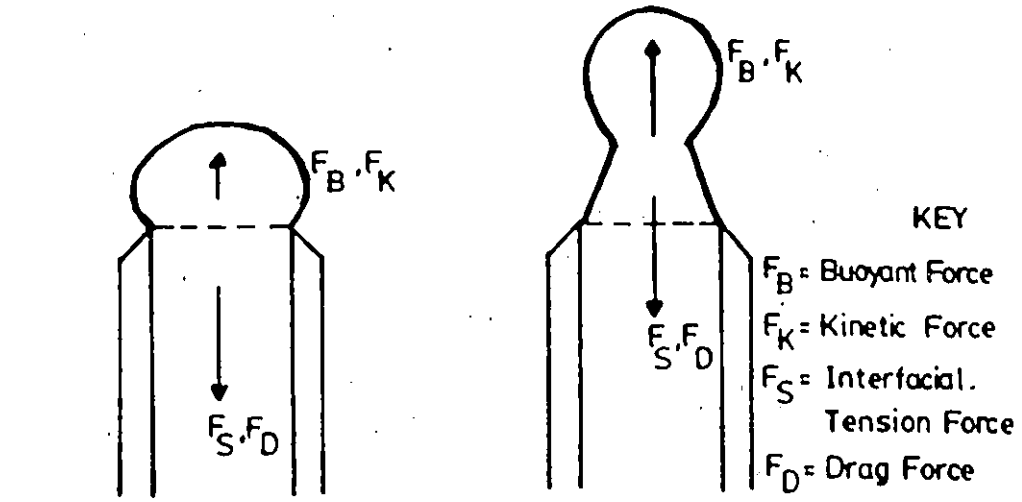

FIGURE 6: DROPLET FORMATION

If V_{FS} is the total liquid volume attached to the nozzle tip at the instant the net force on the forming drop equals zero, the buoyancy force is:

$$F_b = V_{FS}\, g\, \Delta\rho \tag{24}$$

and the interfacial tension force is:

$$F_s = \pi\, \sigma\, D_N \tag{25}$$

At low flow conditions, these would be the only noticeable forces acting on the drop and the volume of the drop formed would be:

$$V_{FS} = \frac{\pi \sigma D_N}{g\ \Delta\rho} \qquad (26)$$

Equation (26) indicates that the droplet volume will depend on the interfacial tension, nozzle diameter and the difference in densities between the two phases.

Once formed, the drops rise through the continuous liquid until they reach the next plate. The velocity with which the drops move determines the residence time of the dispersed phase between the plates and thus the hold-up. As a simple approach, assume the drops behave as if they were solid spheres travelling at their terminal velocity. The terminal velocity of the drop is expressed by:

$$V_t = \left[\frac{4gD\Delta\rho}{3C_D\rho_c}\right]^{0.50} \qquad (27)$$

Klee and Treybal [25] developed an empirical correlation for a droplet rising or falling in a column.

$$V_t = 38.3\ \rho_c^{-0.45}\ \Delta\rho^{0.58}\ \mu_c^{-0.11}\ D^{0.20} \qquad (28)$$

The length of time the drop stays in suspension between the plates determines its hold-up; due to this, Equations (27) or (28) can be used to measure the effect the system variables have on the hold-up.

3.2 INTERFACIAL PHENOMENA

Two possible regimes can exist when an immiscible liquid phase is added to another liquid containing solids. These are:

1. Distribution of the solid phase into one or the other liquid phase
2. Collection of the solids at the interface between the two liquids

For a particular system, the manner in which the solids distribute themselves is dictated, among other things by their surface properties.

Consider the situation below in which a solid and two immiscible liquid phases are present. The condition for the equilibrium in Figure 7 is:

$$\sigma_{s1} = \sigma_{s2} + \sigma_{12}\cos\theta \tag{29}$$

The contact angle, θ measured through liquid 2 is zero when it is totally wetted by liquid 2 and 180° when it is wetted by liquid 1. Employing Equation (29), the solids distribute themselves according to the following criteria:

$$\frac{\sigma_{s1}-\sigma_{s2}}{\sigma_{12}} > 1 = \cos\theta \text{ ; particles wetted by (2)} \tag{30a}$$

$$\frac{\sigma_{s1}-\sigma_{s2}}{\sigma_{12}} < -1 = \cos\theta \text{ ; particles wetted by (1)} \tag{30b}$$

$$\frac{\sigma_{s1}-\sigma_{s2}}{\sigma_{12}} \leq 1 = \cos\theta \text{ ; particles at interface} \qquad (30c)$$

In most cases, the solids are partially wetted by both phases. It is likely then, that they will stick at the interface (Equation 30c) between the two liquids. For a spherical solid particle, this situation is shown in Figure 8. If the contact angle, θ is less than 90°, the particle will be for the most part in liquid 2 (i.e. θ_2). Conversely, when θ is greater than 90°, the bulk of the solid will reside in liquid 1 (i.e. θ_1).

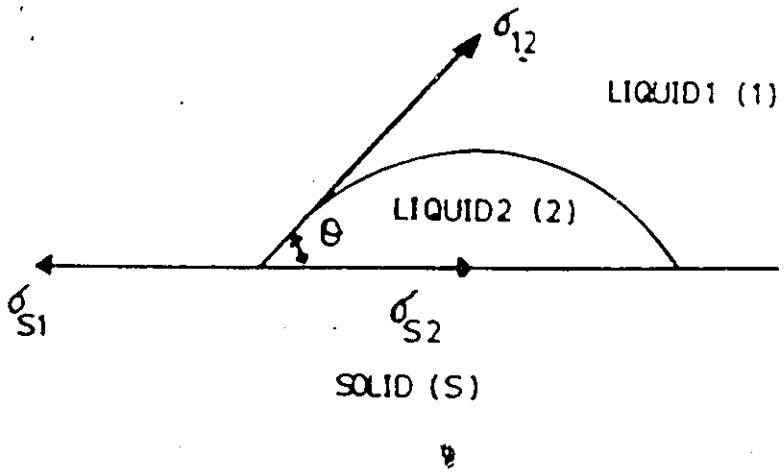

FIGURE 7: EQUILIBRIUM AT A THREE PHASE BOUNDARY

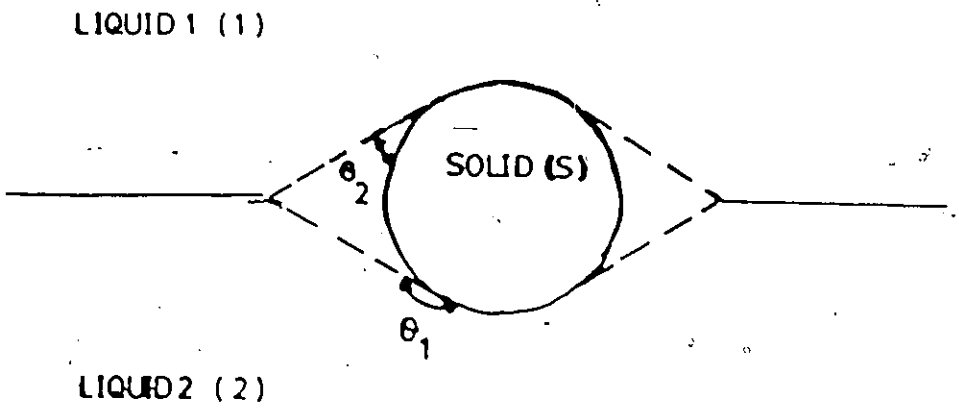

FIGURE 8: SOLID SPHERE SUSPENDED AT INTERFACE

It is agreed by Briggs [26] and others [27,28] that the liquid that wets the solid the more strongly under the conditions of the experiment, tends to become the outside phase; while the less strongly wetting liquid is broken into a drop. The reason for this is not fully understood. A few explanations have been provided; one of them being proposed by Finkle et al [27]. They suggest that when there are enough solid particles to fill the interface, the tendency of the interface to contract will cause it to bend in the direction of the poorly wetting liquid, which makes it easier for the latter phase to become the enclosed phase. Scar-

lett [28] reported that solid particles stabilizing an emulsion protruded largely into the outer liquid, thus indicating better wetting by that phase. It was also hypothesized that emulsion droplets having the particles chiefly on the outside would be better protected from coalescence than those with particles on the inside. In this way, an emulsion of the poorly wetted phase is stabilized.

Chapter IV

EXPERIMENTAL

Experimental runs involved measurement of the dispersed phase hold-up (volume fraction) and drop sizes. It should be noted that the organic phase was maintained as the continuous phase while the aqueous was broken into droplets and formed the dispersed phase.

Since the system studied was previously untested, equipment modifications had to be made to the column throughout the course of the experimental programme. The most important of these was the redesigning of the organic and pulse inlets to prevent the formation of stable emulsions. The probability of this occurring increased as the flow rate or pulse conditions increased. It was thought that emulsion formation was caused by the pulsating flow of the organic phase. A pressure dampener was therefore placed in the organic feed line. The organic distributor was also replaced to reduce emulsion formation. The original design resembled a shower head nozzle which increased emulsion formation at higher flow rates. To alleviate this problem, a polypropylene 'T' fitting was used as the distributor. This increased the inlet area and directed the flow outwards to facilitate coalescence. As the frequency of the pulse was increased again

stable emulsions were formed. The original 1.90 cm inlet was replaced by a 3.80 cm inlet to reduce the turbulence created by the sudden change in cross sectional area at the entrance.

When solids were added to the aqueous phase, it was necessary to increase the fractional free area on the plates to reduce the amount of settling in the column. The amplitude was increased during the course of the study to increase the turbulence in the column. By doing this, it was hoped that operation in the dispersion or emulsion region would be achieved.

4.1 VARIABLES

The variables studied were: pulse frequency, aqueous flow rate and organic flow rate. To extract as much information as possible from the experiments concerning the relationship between the hold-up and these variables, a model was fitted to the data. Since no adequate theoretical relationship was known for the entire operating region studied, an empirical approach was taken. A modified linear model was used based on the results obtained by Bell and Babb [16]. The proposed model for the hold-up X_d was:

$$X_d = B_0 + B_1X_1 + B_2X_2 + B_3X_3 + B_4X_1^2 + B_5X_2^2 + B_6X_3^2 + B_7X_1X_2 + B_8X_1X_3 + B_9X_2X_3 + B_{10}X_1^2X_2 + B_{11}X_1X_2^2 \quad (31)$$

Once the data were collected, a linear least squares analysis was performed to obtain estimates of the various parameters (B_i). Then, by using an estimate of the pure error variance, 95% confidence intervals were calculated and the parameters that were not significant (i.e. those whose values included zero) were dropped from the model. Further analysis of residuals and other statistical tests enabled the final form of the model to be found.

The variables studied and the way in which they are varied determine the usefulness of the final model. Some experience is necessary in order to define important variables as well as the test regions to adequately describe the effect these variables have on the response value. The choice of test regions also defines the area of applicability of the models [29]; they are most accurate within this region and should not be used outside of it. The way in which the variables are changed from run to run affects the accuracy of the model and its parameters [30]. Considering all of these points, it is advisable that some plan or design be followed to obtain the best model for the experiments performed.

In this case, an incomplete three-level factorial design was chosen since it was economical in the number of tests to be performed. This proved to be an advantage as when solids were added both the stator and rotor in the Monyo pump were subject to severe erosion which proved to be a substantial

problem. The factorial design also provided parameter estimates that were to a large extent mutually uncorrelated and with minimum variance. This design required that three equally spaced values for each operating variable be chosen. The operating variables and their levels are listed in Table 2.

Table 2: OPERATING CONDITIONS

VARIABLE	OPERATING LEVEL		
	LOWER	MIDDLE	UPPER
Frequency of Pulsation (cycles/min)	22.0	31.0	40.0
Aqueous Flow Rate (ml/min)	Levels were different for each DATA SET (see RESULTS)		
Organic Flow Rate (ml/min)	379.3	579.1	778.8

In order to avoid round-off error in later calculations, coded variables X_1, X_2, and X_3 were used to represent frequency of pulse, aqueous flow rate and organic flow rate respectively. These were calculated using the expression below:

$$X_i = \frac{\left(\begin{matrix}\text{value of operating} \\ \text{variable } i\end{matrix}\right) - \frac{1}{2}\left(\begin{matrix}\text{its upper} \\ \text{limit}\end{matrix} + \begin{matrix}\text{its lower} \\ \text{limit}\end{matrix}\right)}{\frac{1}{2}\left(\begin{matrix}\text{its upper} \\ \text{limit}\end{matrix} - \begin{matrix}\text{its lower} \\ \text{limit}\end{matrix}\right)} \qquad (32)$$

For each coded variable, -1 represents the lowest value of the operating variable tested, 0 the intermediate value and +1 the highest value. This nomenclature will be used throughout subsequent analysis and discussion of results. Further details concerning the calculation of the statistics used, tests performed and the design followed are described in Appendix A.

4.2 SYSTEM STUDIED

The organic phase was maintained as the continuous phase in all experiments, it contained 5% by volume ALAMINE 336 (extractant), 5% by volume ISODECANOL (modifier) and 90% by volume SHELL 140 (diluent). The aqueous phase consisted of distilled water containing 30 g/l of ammonium sulphate with sulphuric acid added to adjust the pH to 1.7. The physical properties of the solutions are presented in Table 3.

Initially, it was hoped to use a spent leach solids from uranium extraction to prepare the slurry phase. This was not possible to carry out due to Atomic Energy of Canada regulations. Consequently, as the spent solids contained mainly silica quartz, a sand blasting material (Silica 70) was used to make up the slurry. The specific gravity of this material was found to be 2.05. This was measured by determining the volume and weight of a graduated cylinder containing sand and water. A size analysis of the material as it was

Table 3: PHYSICAL PROPERTIES OF SYSTEM AT 25°C

	Density (kg/m^3)	Viscosity $\times 10^3$ (Pa.s)	Surface Tension (mN/m)
(I)Organic Phase 5%ALAMINE336 5%ISODECANOL 90%SHELL 140	807	1.744	25.2
(II)Aqueous Phase 30g/l $(NH_4)_2 SO_4$ pH 1.7	1011	0.932	51.3
Interfacial Tension between (I) and (II)			10.6

Density measured using an Anton Paar Digital Densitometer Model DMA 60 (Austria)

Viscosity measured using Cannon-Fenske Routine Viscometer

Surface and Interfacial Tension measured using Fisher Model 215 Autotensiomat Surface Tension Analyser

used in most of the experiments is given in Table 4. Later, experiments were performed using the smallest size fraction of the material described above (i.e.-125μm), its screen analysis is given in Table 5.

Table 4: SIZE ANALYSIS OF SILICA 70

Size (μm)	%Retained
+250	3.3
+180-250	40.2
+125-180	36.9
-125	19.6

Table 5: SIZE ANALYSIS OF FINE FRACTION OF SILICA 70

Size (μm)	%Retained
+106-125	42.9
+ 90-106	26.4
+ 75- 90	18.7
+ 38- 75	9.5
- 38	2.5

4.3 APPARATUS

A schematic of the apparatus is given in Figure 9, column dimensions are shown in Table 6.

The column consisted of one section of plexi glass 167.7 cm long. Inside the column, 17 stainless steel perforated plates were mounted on a single stringer rod and separated by spacers 7.62 cm in length. Two sets of plates were used,

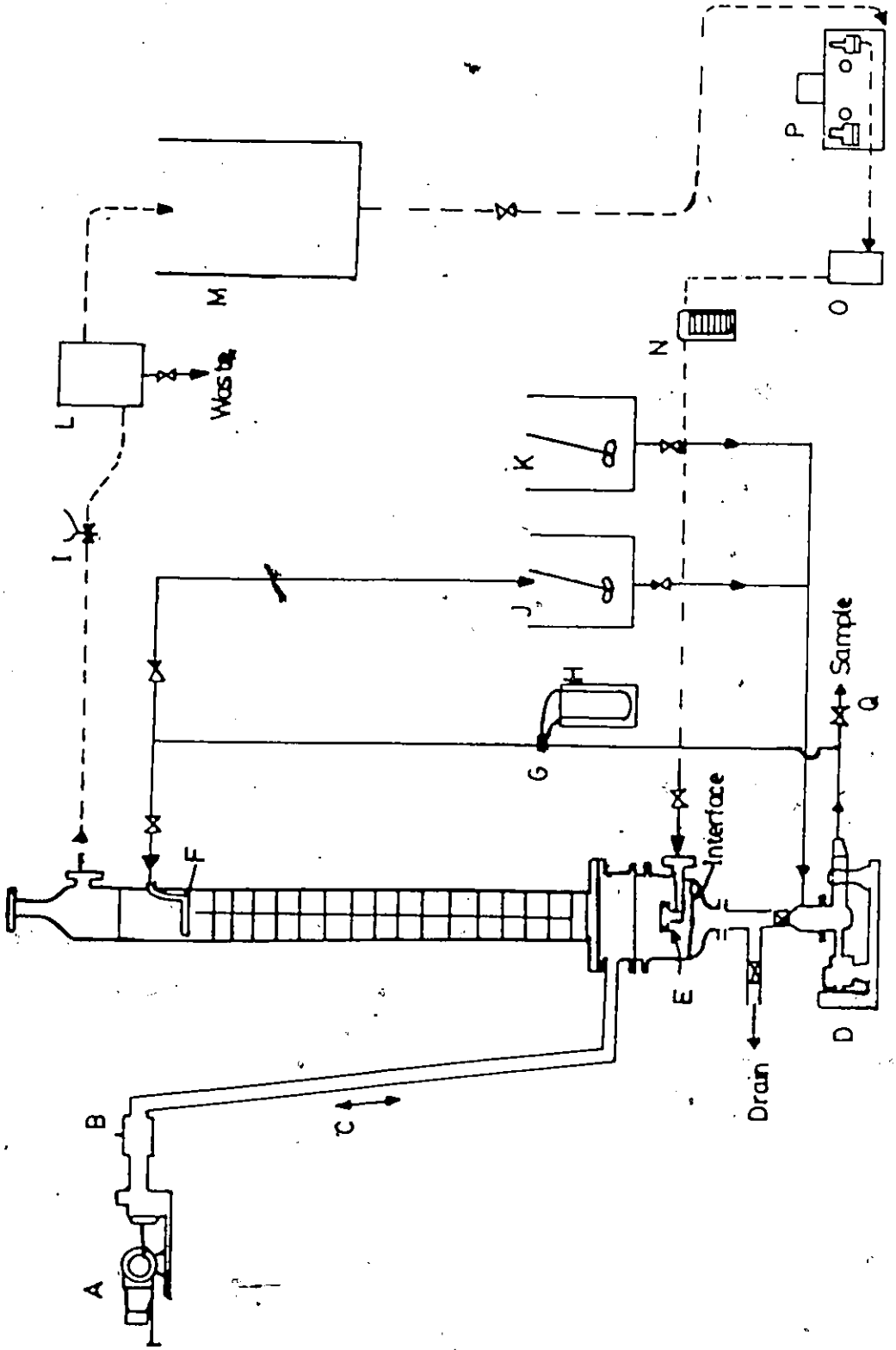

FIGURE 9: SCHEMATIC DIAGRAM OF EQUIPMENT

KEY

A	Pulse Pump
B	Vent
C	Pulse Leg
D	Aqueous Pump
E	Organic Distributor
F	Aqueous Distributor
G	Orifice Meter
H	Manometer
I	Solenoid Valve
J	Slurry Recycle Tank
K	Aqueous Tank
L	Settler
M	Organic Tank
N	Filter
O	Pulse Dampener
P	Organic Pump
Q	Pulp Sample Removal
——	Aqueous Flow
- - -	Organic Flow

Table 6: PULSED COLUMN DIMENSIONS

Dimensions given in cm unless otherwise specified

Column I.D.	10.160
Plate Diameter	10.097
Plate Thickness	0.166
Sieve Hole Diameter	0.359
Plate Spacing	7.620
Central Rod O.D.	0.953
Aqueous Distributor O.D.	6.580
Number of Holes in Plates Cartridge 1	164
Cartridge 2	191
Plate Free Area Cartridge 1	20.9%
Cartridge 2	24.4%
Distance Between 1st Plate and Organic Distributor	23.8
Distance Between 17th Plate and Aqueous Distributor	11.3
Effective Height of Column (one plate height above 17th plate to one plate height below 1st one)	141.0
Effective Volume	11119 ml

plate specifications are given in Table 6. The ends of the main column were connected by flanges to phase disengagement sections. The top section, which includes a calming area is 23.5 cm in length. Since the aqueous phase was dispersed throughout this study, the active aqueous/organic interface was in the lower disengagement section, see Figure 9.

The aqueous phase entered the column through a stainless steel distributor. To move the aqueous phase through the circuit, a Robbins and Meyers Monyo Pump was used. The flow was regulated by changing the speed of rotation of the pump. After some experimentation, the output was found to decrease for the same rotational speed. Deterioration in output occurred for the most part when slurry tests were performed. The sand was found to erode both the stainless steel rotor and the Buna-N stator. These had to be replaced one and four times respectively throughout the course of the experimentation. The rate of this deterioration was sharply reduced by decreasing the rotor speed. It is recommended that an oversized pump be used in the future so that for a given flow rate the speed of the rotor could be reduced, which would reduce equipment wear. To ensure a steady flow rate, an Orifice Meter was designed and installed near the outlet of the pump (see Appendix B for description and calibration).

The organic phase, which was the continuous phase entered through a polypropylene 'T' fitting. Flow was provided by a Milton Roy Controlled Volume Diaphragm pump (see Appendix B for calibration). The output was found to be very steady and did not vary appreciably over the course of the experiments so no volumetric measuring device was needed.

The pulsing action was provided by a modified Denver diaphragm pump. Pulse frequency, which is the time required for a full up and down movement was varied by changing the

speed of rotation of the cam. The total vertical displacement of the fluid in the column, known as the amplitude was altered by changing the length of the connecting rod. The pulse entered the column between the organic distributor and the first plate. Tygon tubing (3.80 cm outside diameter), was used to connect it to a stainless steel fitting on the column.

A Pentax K1000 35 mm camera was used to obtain still photographs of the drops within the column. It was placed on a tripod at a distance of 45 cm in front of the column. To provide illumination, a 1000 watt tungsten flood light was placed about 75 cm behind the column. A diffusing screen was attached directly behind the column to ensure uniform lighting in the field of view. With the conditions used in this study, it was found that an aperature of f16 and a shutter speed of 1/250 sec using 125 ASA film provided the best results.

4.4 PROCEDURE

The aqueous feed solution was prepared by dissolving 30 g/l of ammonium sulphate in distilled water. Sulphuric acid was then used to adjust the pH to 1.7. In later experiments, no acid was added so that the aqueous phase pH was approximately 5.5. Organic solvent was obtained from E.M.R. already pre-equilibrated with 5% sulphuric acid.

For the initial studies with a clear aqueous feed the procedure followed is outlined below:

1. The bottom settling region was filled to about 3-4 cm above the final interface level with the aqueous phase.
2. The rest of the column was filled with the organic phase. The pulse leg was only partially filled with organic so that the pulse could be observed and its frequency measured during the course of the experiment.
3. Organic flow rate, pulse frequency and amplitude were adjusted to their desired value.
4. The aqueous phase pump was turned on to draw solution from the bottom settling region of the column and recycle it back to the top.
5. After 15 minutes, the interface was adjusted to a previously established mark. Pictures of the dispersion were then taken.
6. At the end of 30 minutes, the aqueous pump and its inlet valve were shut to initiate a hold-up measurement.
7. The organic and pulse pumps were operated a further 5 minutes to ensure all aqueous in the column settled to the bottom interface.
8. A hold-up measurement was then made by draining the column and measuring the volume necessary to allow the

interface to reach the previously established mark. The fractional hold-up was obtained by dividing the volume measured by the effective volume.

When sand was added to the aqueous phase it was necessary to modify the procedure. In this case, the steps followed were:

1. The first three steps were the same as those described previously.
2. The recycle tank (J in Figure 9) was filled with aqueous solution, the aqueous pump was then started to recycle this solution.
3. The mixer was turned on and an appropriate amount of sand added to the tank, an excess amount of sand was added to account for any settling occurring in the equipment.
4. The aqueous pump was allowed to recycle the slurry for 10 minutes after which time the valve to the tank was closed and that to the column opened.
5. While the pump was filling the column with the slurry, solution was withdrawn from the bottom of the column to ensure a constant interface level at 5 cm above the established mark. This additional volume was provided to allow for later sampling.
6. When most of the solution from the tank was pumped into the column, the valve at the bottom of the tank was closed while that at the bottom of the column was

opened; the pump was then recycling the slurry in the column.

7. About 1-2 hours was required to reach equilibrium, at which time the weight percent of solids being recycled was relatively constant at 10.6 +/- 0.5 (NOTE: weight percent solids was obtained by measuring the density of solutions withdrawn from a sampling valve, Q in Figure 9). At this time the interface was adjusted to the established mark and pictures were taken.

8. After 15 minutes the aqueous pump was shut off and the hold-up measured as outlined previously.

4.5 DROP SIZE MEASUREMENTS

During the experiments, the compartments between the 6th and 7th plates were photographed. These photographs were developed and their negatives enlarged to approximately 2-3 times their normal size and then examined using a Kontron type Zeiss Particle Size Analyser. An analysis of drop minimum and maximum diameters was obtained by placing the enlarged photograph on a magnetized tablet and circling each drop observed. The number of drops circled in each experiment varied depending on the operating conditions. A detailed description of the measuring procedure is given in Appendix C.

Chapter V

RESULTS

Three sets of experiments were carried out without solids. These were performed to test the equipment and to establish the operating conditions for subsequent slurry tests.

The first tests were carried out at a low amplitude (0.75 cm) and with the first set of plates (20.9% plate free area). Experimental conditions used as well as the hold-up results obtained are summarized in TABLE 7. It should be noted that the conditions were not exactly as specified by the design, levels for X_2 should have been -1,0, and +1. This discrepancy was not noticed until later when an orifice meter was installed to measure the aqueous flow rate. Also note that some repeated runs other than those required by the design were carried out. These were used in addition to other non-slurry replicates to obtain a pooled estimate of the pure error variance (i.e.experimental error). After performing an analysis of the data as outlined in Section 4.1 the fitted model was:

$$X_d = 2.41 - 0.07X_1 + 1.30X_2 - 0.32X_2^2 - 0.18X_3^2 - 0.16X_1X_2 - 0.13X_1^2X_2 \quad (33)$$

Observed and predicted values for this DATA SET are plotted in Figure 11. The associated parameter's 95% confidence intervals as well as a plot of the residuals versus each of the operating variables is available in Appendix D. The results from a significance test suggests that any inadequacy in the fitted model is not significantly larger than the experimental error; thus the model was accepted.

Table 7: OPERATING CONDITIONS AND RESULTS FOR DATA SET I

Plate free area was 20.9% and amplitude 0.75 cm for this set of data. Aqueous flow rates were 962.8, 1175.4 and 1307.6 ml/min for X_2 = -1, 0.2332 and +1 respectively.

X_1	X_2	X_3	HOLD-UP (%)	
-1	-1	0	1.42	1.45
1	-1	0	1.34	
-1	1	0	4.44	
1	1	0	3.51	3.89
-1	0.2332	-1	2.60	
1	0.2332	-1	2.38	
-1	0.2332	1	2.72	
1	0.2332	1	2.39	2.55
0	-1	-1	1.32	
0	1	-1	3.89	
0	-1	1	1.30	
0	1	1	3.73	
0	0.2332	0	2.74	
0	0.2332	0	2.80	
0	0.2332	0	2.67	

The results shown in Table 8 were obtained with similiar operating values as shown in Table 7. In this case, the plates with the larger plate free area were used (see Table

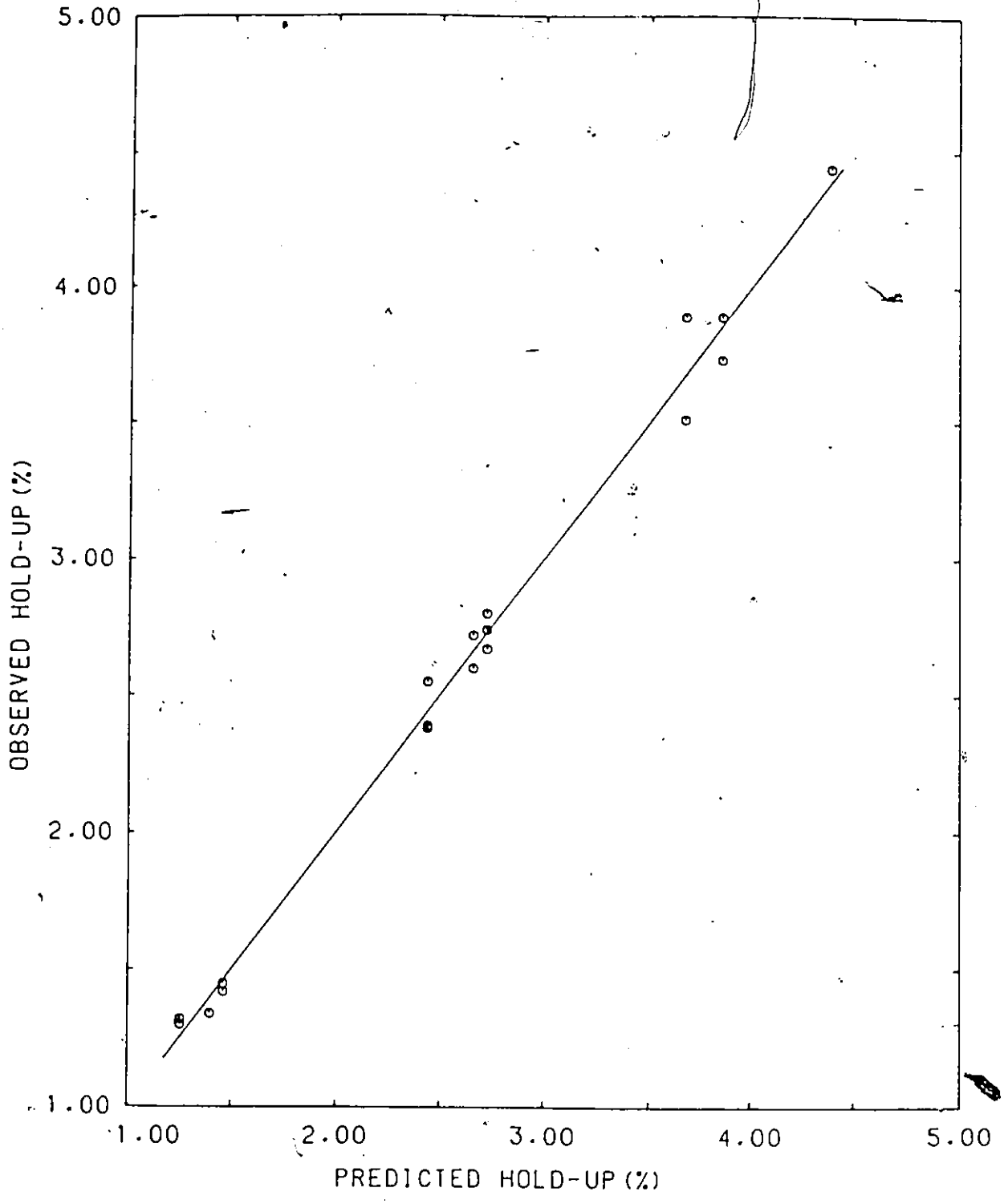

FIGURE 11: OBSERVED AND PREDICTED VALUES OF HOLD-UP FOR DATA SET 1

6). The 'best' model that described the data in Table 8 was:

$$X_d = 4.45 - 1.06X_1 + 1.63X_2 + 0.12X_3 - 0.19X_1^2 - 0.15X_3^2 - 0.14X_1X_2 - 0.24X_1^2X_2 + 0.27X_1X_2^2 \quad (34)$$

Using a significance test, the model error was found to be smaller than the experimental error indicating the adequacy of the model. Observed and predicted values are plotted in Figure 12, while residual plots are located in Appendix D.

Table 8: OPERATING CONDITIONS AND RESULTS FOR DATA SET II

In this set of data plates of 24.4% free area were used, the amplitude was 0.75 cm. The aqueous flow rates were 523.4, 787.5 and 1045.8 ml/min for X_2 = -1, 0 and +1 respectively.

X_1	X_2	X_3	HOLD-UP (%)
-1	-1	0	3.54
1	-1	0	2.24
-1	1	0	6.61
1	1	0	4.74
-1	0	-1	4.92
1	0	-1	2.97
-1	0	1	5.37
1	0	1	3.09
0	-1	-1	2.55
0	1	-1	5.90
0	-1	1	2.84
0	1	1	6.01
0	0	0	4.40
0	0	0	4.51
0	0	0	4.34

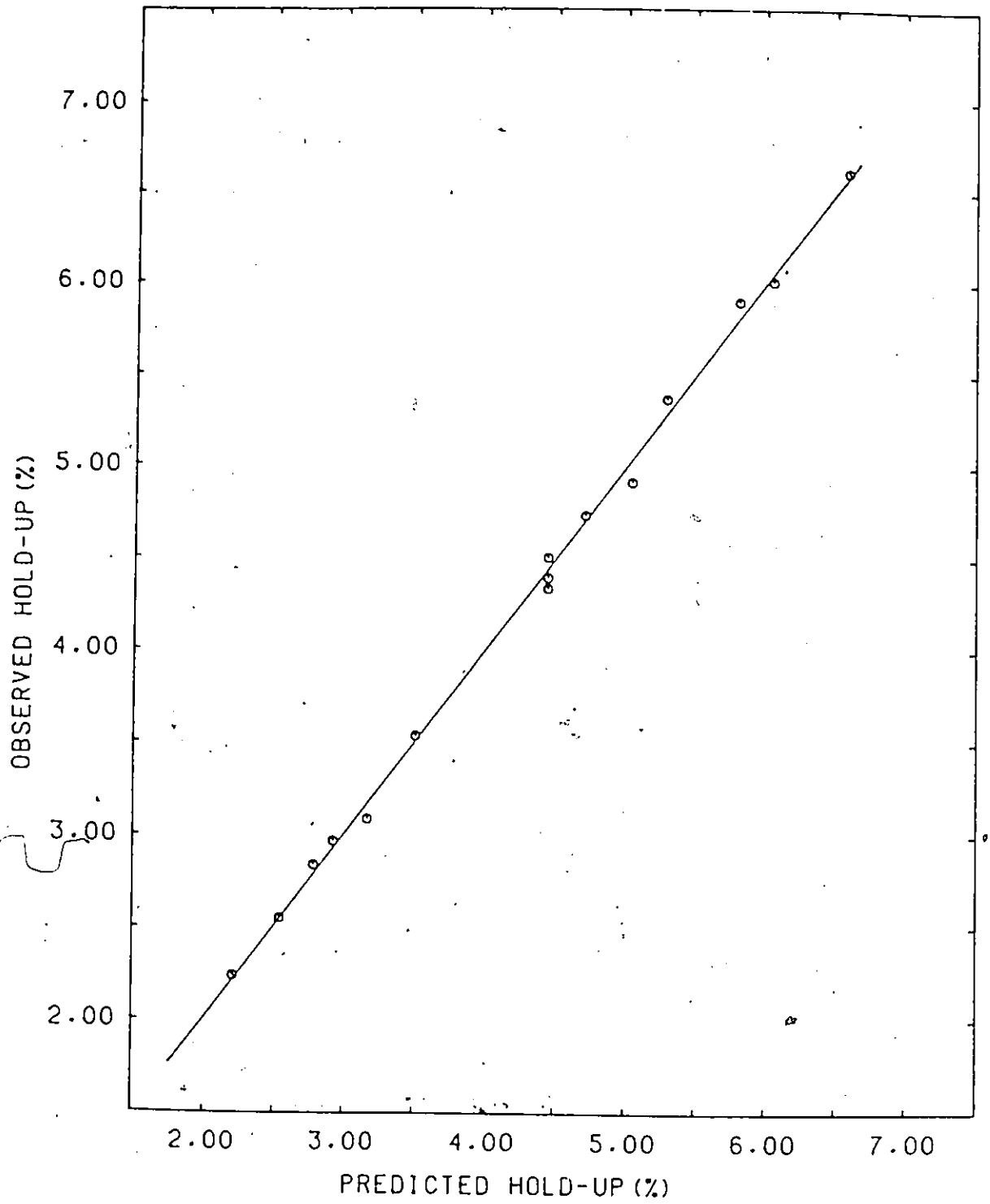

FIGURE 12: OBSERVED AND PREDICTED VALUES OF HOLD-UP FOR DATA SET 11

The next set of data was obtained with the pulse amplitude increased to 2.55 cm; conditions employed and results for DATA SET III are presented in Table 9. The fitted equation obtained for DATA SET III was:

$$X_d = 4.08 + 0.48X_1 + 1.15X_2 + 0.09X_3 + 0.48X_1^2 + 0.17X_2^2 + 0.22X_1X_2 + 0.18X_1^2X_2 \quad (35)$$

In Figure 13, observed and predicted values obtained are shown (Note: residuals appear in Appendix D). The test ratio suggests that any inadequacy in the fitted model is not significantly larger than the experimental error.

Table 9: OPERATING CONDITIONS AND RESULTS FOR DATA SET III

The second set of plates were used (i.e.plate free area 24.4%) with a pulse amplitude of 2.55 cm. Aqueous flow rates were 792.0, 1049.6 and 1303.3 ml/min for X_2 = -1, 0 and +1 respectively.

X_1	X_2	X_3	HOLD-UP (%)		
-1	-1	0	3.14	3.12	
1	-1	0	3.74	3.53	3.76
-1	1	0	5.29	5.38	
1	1	0	6.69	6.90	
-1	0	-1	4.13	4.04	
1	0	-1	4.78	4.63	5.10
-1	0	1	4.02	4.22	
1	0	1	5.00	5.31	5.22
0	-1	-1	2.94	3.01	
0	1	-1	5.44	5.29	
0	-1	1	3.36	3.05	
0	1	1	5.51	5.30	
0	0	0	3.27	3.25	
0	0	0	3.24	3.24	
0	0	0	3.28	3.27	

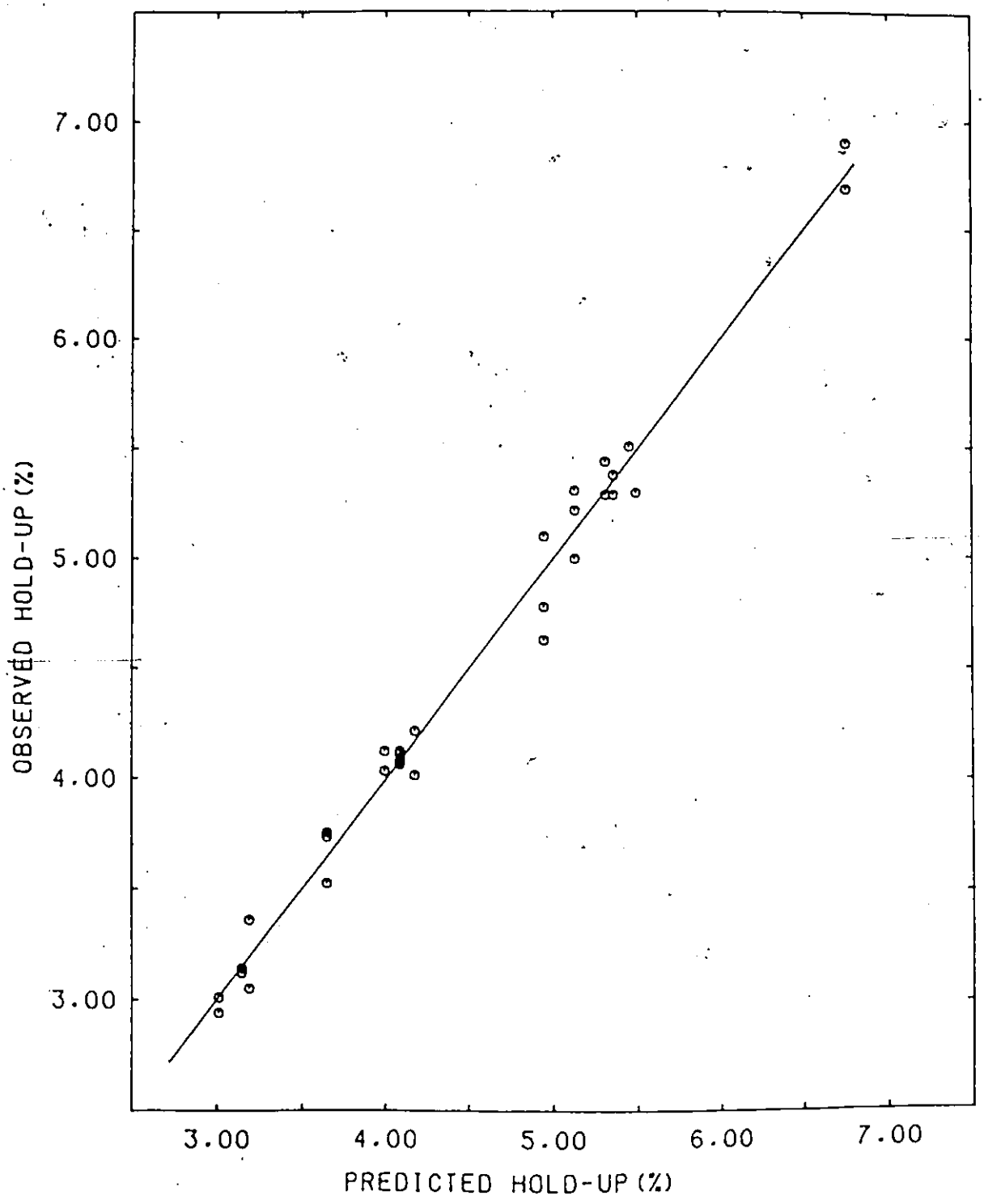

FIGURE 13: OBSERVED AND PREDICTED VALUES OF HOLD-UP FOR DATA SET III

The last experimental design was performed at the same conditions as DATA SET III; but in this case, sand was added to the aqueous phase. Solids concentration in these tests varied from 10.1 to 11.1 percent by weight. A narrower range was not possible with the experimental set-up employed. The results are shown in Table 10. The equation obtained for DATA SET IV was:

$$X_d = 2.75 + 0.05X_1 + 0.82X_2 + 0.30X_1^2 + 0.26X_2^2 - 0.15X_1X_2 \qquad (36)$$

A test of significance indicates that the model is adequate in describing the data. A plot showing the goodness of fit appears as Figure 14 (residual plots are provided in Appendix D).

Other tests performed to evaluate the effects of particle size and pH of the aqueous phase are summarized in Table 11.

Using the Zeiss Particle Size Analyser the Sauter mean diameter, D_{32} was obtained, the results are provided in Table 12.

Table 10: OPERATING CONDITIONS AND RESULTS FOR DATA SET IV

The second plate cartridge was used (i.e. 24.4% plate free area) with a pulse amplitude of 2.55 cm. Aqueous slurry flow rates were 789.0, 1044.0 and 1306.7 ml/min for X_2= -1, 0 and +1 respectively.

X_1	X_2	X_3	HOLD-UP % (PULP DENSITY)	
-1	-1	0	2.32(11.1)	2.35(10.3)
1	-1	0	2.75(10.2)	2.51(10.1)
-1	1	0	4.32(10.8)	
1	1	0	4.10(11.0)	3.82(10.2)
-1	0	-1	2.81(10.7)	
1	0	-1	3.25(10.1)	2.95(10.3)
-1	0	1	3.02(10.4)	
1	0	1	3.44(10.3)	
0	-1	-1	2.42(10.2)	2.07(10.5)
0	1	-1	3.80(10.5)	
0	-1	1	2.17(10.4)	
0	1	1	3.92(10.2)	
0	0	0	2.84(10.8)	
0	0	0	2.64(10.9)	
0	0	0	2.65(11.1)	

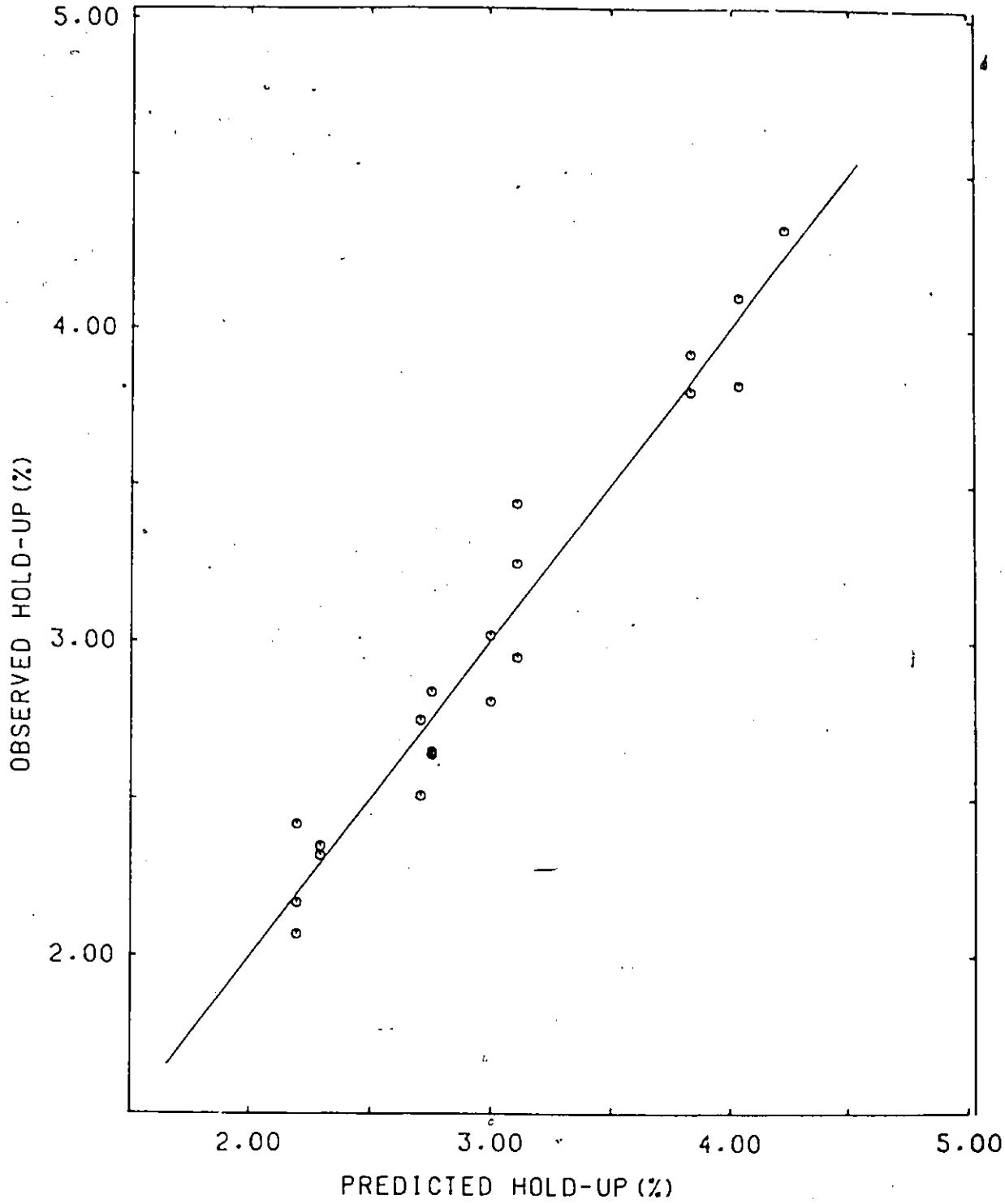

FIGURE 14: OBSERVED AND PREDICTED VALUES OF HOLD-UP FOR DATA SET IV

Table 11: EFFECT OF PARTICLE SIZE AND AQUEOUS PHASE pH ON HOLD-UP

Plate free area was 24.4%, pulse amplitude 2.55 cm and $X_2 = -1$ and $X_3 = 0$.

AQUEOUS PHASE CONDITIONS	X_1	HOLD-UP % (PULP DENSITY)	
Sand in pH 1.7	-1	2.32(11.1)	2.35(10.3)
	0	1.93(10.5)	2.15(11.0)
	1	2.75(10.2)	2.51(10.1)
Fine Sand in pH 1.7	-1	2.65(10.2)	3.06(11.1)
	0	2.53(10.3)	2.09(10.7)
	1	2.70(11.1)	2.19(10.9)
Sand in pH 5.5	-1	2.47(10.2)	2.26(10.8)
	0	2.11(10.6)	2.07(10.5)
	1	2.38(10.6)	2.27(10.4)

NOTE: 'Sand' refers to original material whose size analysis appears in TABLE 4. 'Fine sand' refers to material in Table 5.

Table 12: DROP SIZES FOR CLEAR AQUEOUS AND SLURRY FEED EXPERIMENTS

OPERATING CONDITIONS			CLEAR AQUEOUS		SLURRY AQUEOUS	
X_1	X_2	X_3	No.of Drops	D_{32} (cm)	No.of Drops	D_{32} (cm)
-1	-1	0	*338	0.414	*485	0.502
-1	1	0	*215	0.468	*303	0.592
-1	0	-1	138	0.448	*298	0.540
0	1	1	151	0.449	144	0.483
0	0	0	142	0.351	*312	0.473
0	0	0			*546	0.494
1	-1	0	260	0.239		
-1	0	1			136	0.557
1	0	1			133	0.424
0	-1	1			124	0.504

NOTE. Data points indicated with * were obtained by pooling the results of more than one picture of the same experiment.

Chapter VI

DISCUSSION

6.1 SOLIDS FREE AQUEOUS TESTS

Discussion of results of the hold-up are based on the linear correlations obtained. DATA SETS I and II were obtained from initial testing of the column and are useful in describing the effect plate free area has on the dispersed phase hold-up. The effect of amplitude on the hold-up is obtained by comparing DATA SETS II and III. However, as these three sets of experiments were not carried out at the same aqueous flow rates, a direct comparison of the equations derived was not possible. To overcome this, the models were evaluated at an aqueous flow rate common to all three DATA SET regions, this being 1000 ml/min. At this flow rate the models for each data set become:

DATA SET I

$$X_d = 1.59 - 0.02X_1 - 0.18X_3^2 \qquad (37)$$

DATA SET II

$$X_d = 5.79 - 0.99X_1 + 0.12X_3 - 0.39X_1^2 - 0.15X_3^2 \qquad (38)$$

DATA SET III

$$X_d = 3.88 + 0.43X_1 + 0.09X_3 + 0.44X_1^2 \qquad (39)$$

In these cases, the variation due to organic flow rate (i.e. X_3) was found to be negligible compared to the experimental error (see Table 13). The drag on the drops due to the moving organic phase had no noticeable effect in the experimental range on drop formation or the terminal velocity of the aqueous drops. This was also reported by Sehmel and Babb [10] and Fernandes [36].

Hold-up profiles of DATA SETS I and II are shown in Figure 15 as a function of pulse frequency (i.e. X_1). It is evident that the increase in the plate free area for DATA SET II has greatly affected the hold-up. With the smaller free area, the column appears to be operating at the boundary between the mixer-settler and emulsion zones, this being reflected by the stable hold-up behaviour as a function of the frequency (i.e. X_1). Results for the second set of plates indicate operation in the mixer-settler region since the hold-up decreases with increasing frequency. Instability and phase inversion observed provided evidence of possible flooding for the operating conditions of DATA SET II. The increase in area decreases the velocity with which the dispersed phase is pumped through the column. This effect is analogous to that observed by a decrease in either the frequency or amplitude of the pulse.

The effect of amplitude on the hold-up is illustrated in Figure 16. Low values of pulse intensity (F×A) are repre-

Table 13: PREDICTED DISPERSED PHASE HOLD-UP FOR SOLIDS FREE AQUEOUS TESTS

Aqueous flow rate was 1000 ml/min or X_2 =-0.7842, 0.8247 and -0.1864 for DATA SETS I, II and III respectively.

DATA SET I

X_3 \ X_1	-1	0	+1
-1	1.43(0.23)	1.41(0.12)	1.39(0.20)
0	1.61(0.16)	1.59(0.12)	1.57(0.19)
+1	1.43(0.17)	1.41(0.12)	1.39(0.18)

DATA SET II

	-1	0	+1
-1	6.13(0.24)	5.52(0.18)	4.14(0.24)
0	6.40(0.22)	5.79(0.17)	4.41(0.22)
+1	6.38(0.24)	5.77(0.18)	4.39(0.24)

DATA SET III

	-1	0	+1
-1	3.79(0.12)	3.79(0.11)	4.66(0.11)
0	3.89(0.10)	3.88(0.09)	4.75(0.10)
+1	3.98(0.12)	3.97(0.11)	4.84(0.11)

NOTE. The figures in brackets represent the 95% confidence interval for that prediction

sented by the model predicted for DATA SET II, where the hold-up decreases with increasing F or pulse intensity. The

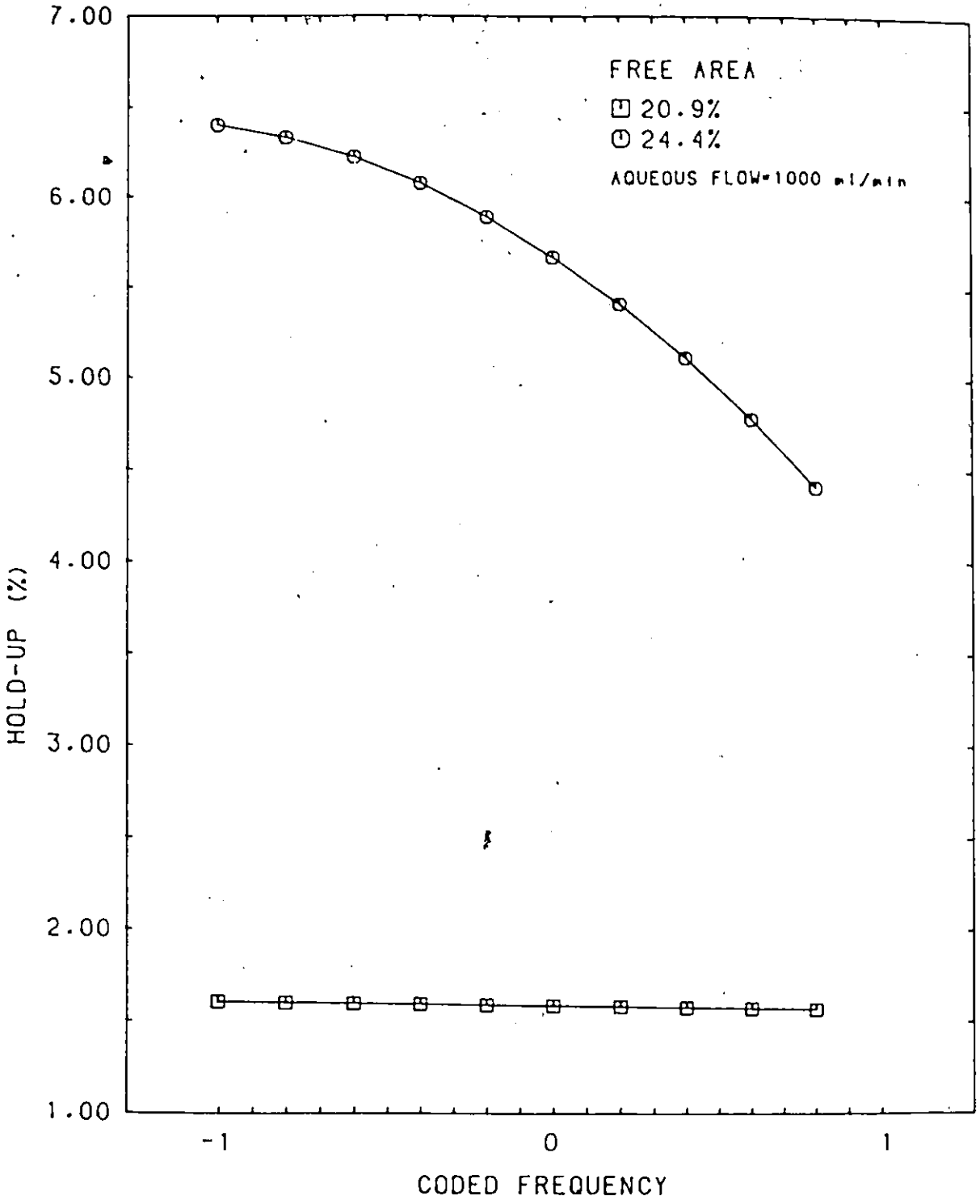

FIGURE 15: PREDICTED HOLD-UP FOR DIFFERENT PLATE FREE AREAS

model for DATA SET III is valid at higher values of (F×A) hold-up first decreased and then increased with increasing pulse intensity. This behaviour indicates operation in the boundary region between the mixer-settler and emulsion regions. It can be said then that the effect of amplitude on the hold-up is similiar to that of frequency. Increases in either of these operating variables increases turbulence in the column and results in variations in the hold-up as predicted by Sehmel and Babb [10]. Therefore a continuous line can be drawn joining the two sets of data, enabling prediction of hold-up at any combination of (F×A) in this range.

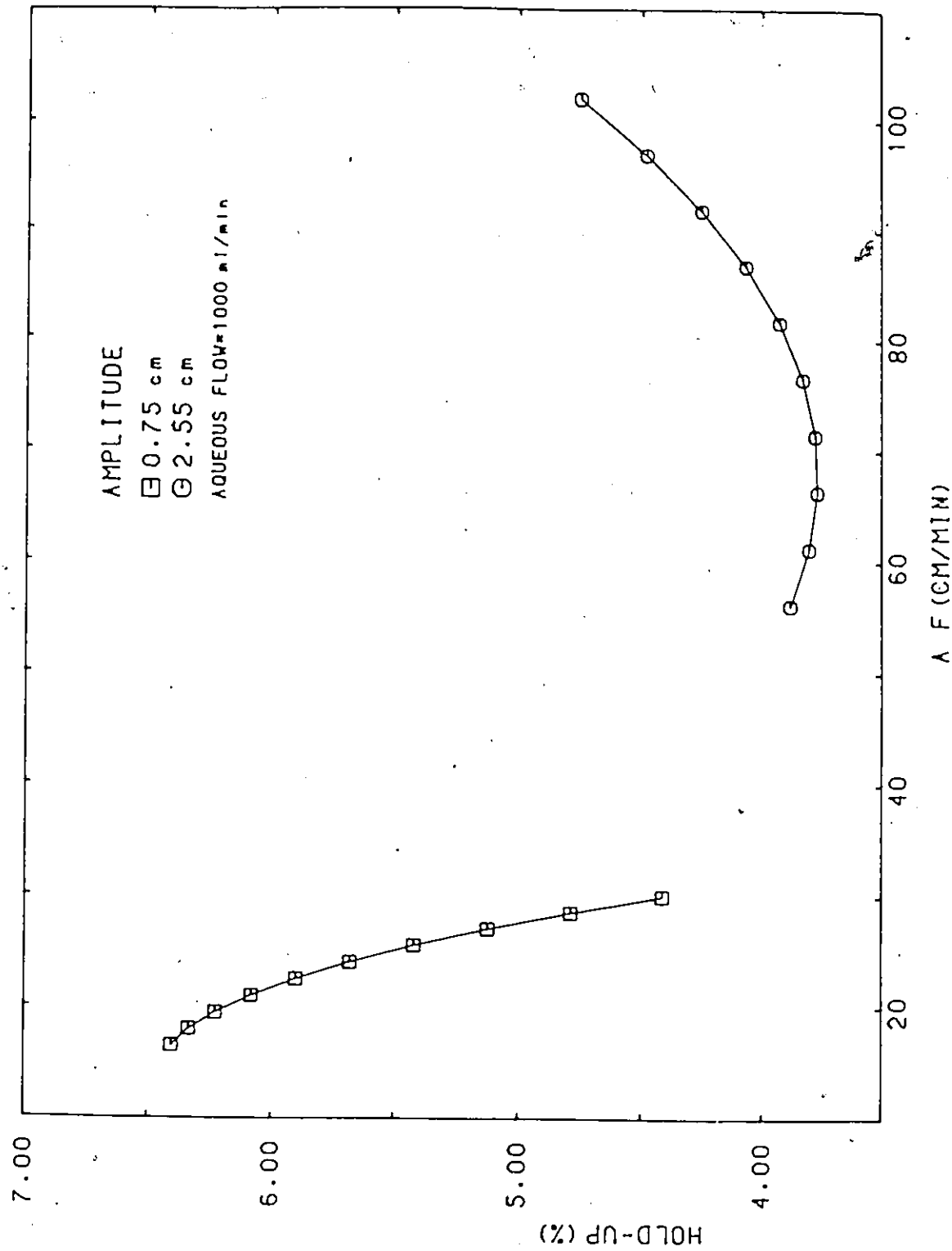

FIGURE 16: HOLD-UP AS A FUNCTION OF PULSE INTENSITY

6.2 SOLIDS ADDITION

6.2.1 OPERATING REGION

Both DATA SETS III and IV were carried out using the same operating conditions the only difference being the addition of solids to the aqueous feed in DATA SET IV. The hold-up profiles predicted by the models for these two data sets are shown in Figure 17 and 18 as a function of frequency and aqueous flow rate. A parabolic relationship is predicted by both models, indicating operation at or near the transition between the mixer-settler and emulsion zones. This transition point (i.e. point of minimum hold-up) differed for the two models. An equation for this minimum was found by differentiating the derived relationships (Equations 35 and 36) with respect to X_1 and equating them to zero. The expressions obtained are plotted in Figure 19 as a function of X_2 (i.e. coded aqueous flow rate). In the region studied, the transition frequency for the clear aqueous tests was lower than that for the slurry tests, indicating that higher frequencies were necessary to attain emulsion operation. As the aqueous flow rate was increased, the transition frequency for the clear aqueous tests remained relatively constant as found by Sehmel and Babb [10]; when solids were present in the aqueous feed this frequency increased with increasing flow rate. If this trend is extended beyond the experimental region, it would suggest the shifting of subsequent operating regions (i.e. emulsion

and flooding) to higher pulse intensities when solids are added.

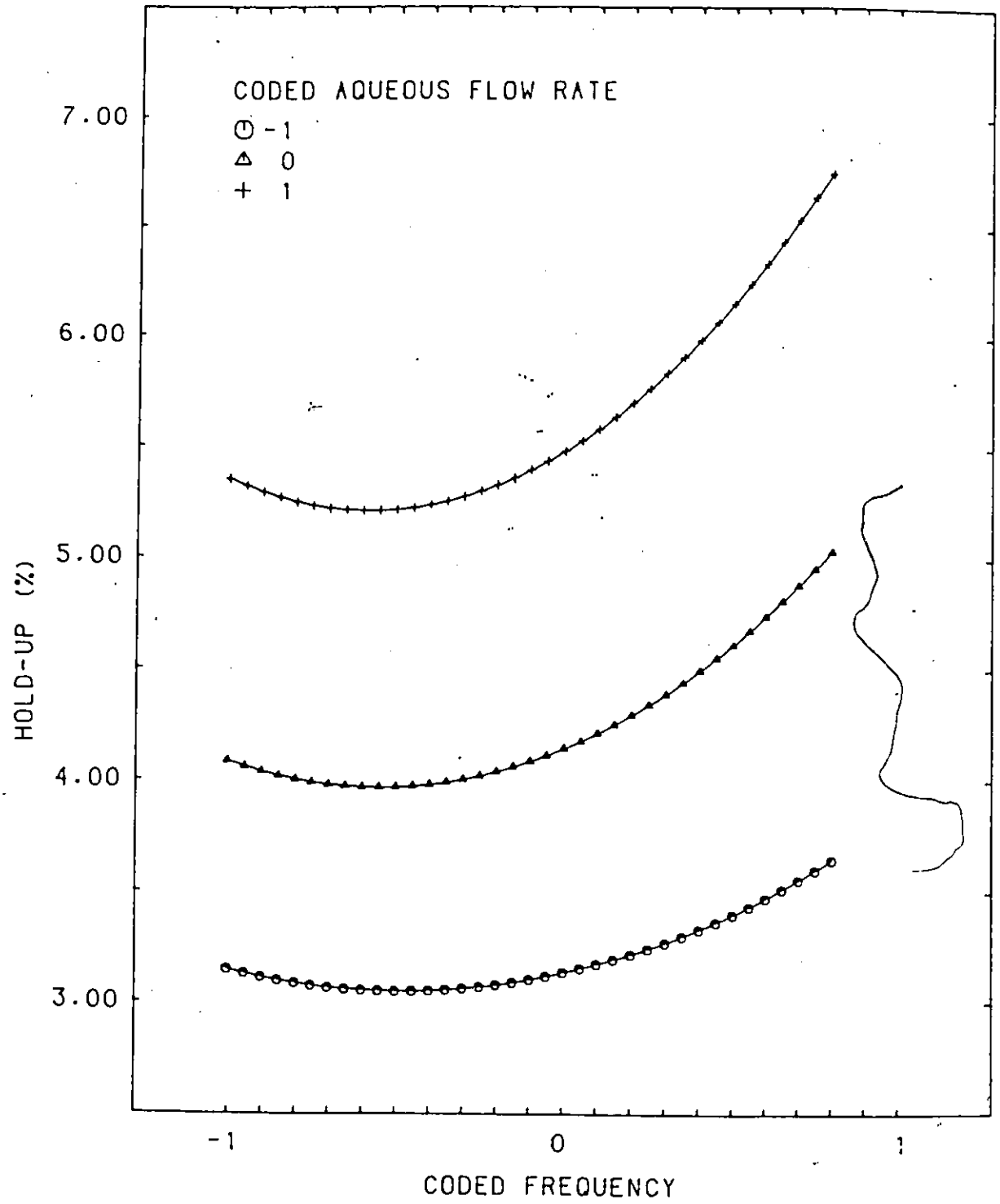

FIGURE 17: PREDICTED HOLD-UP FOR DATA SET III

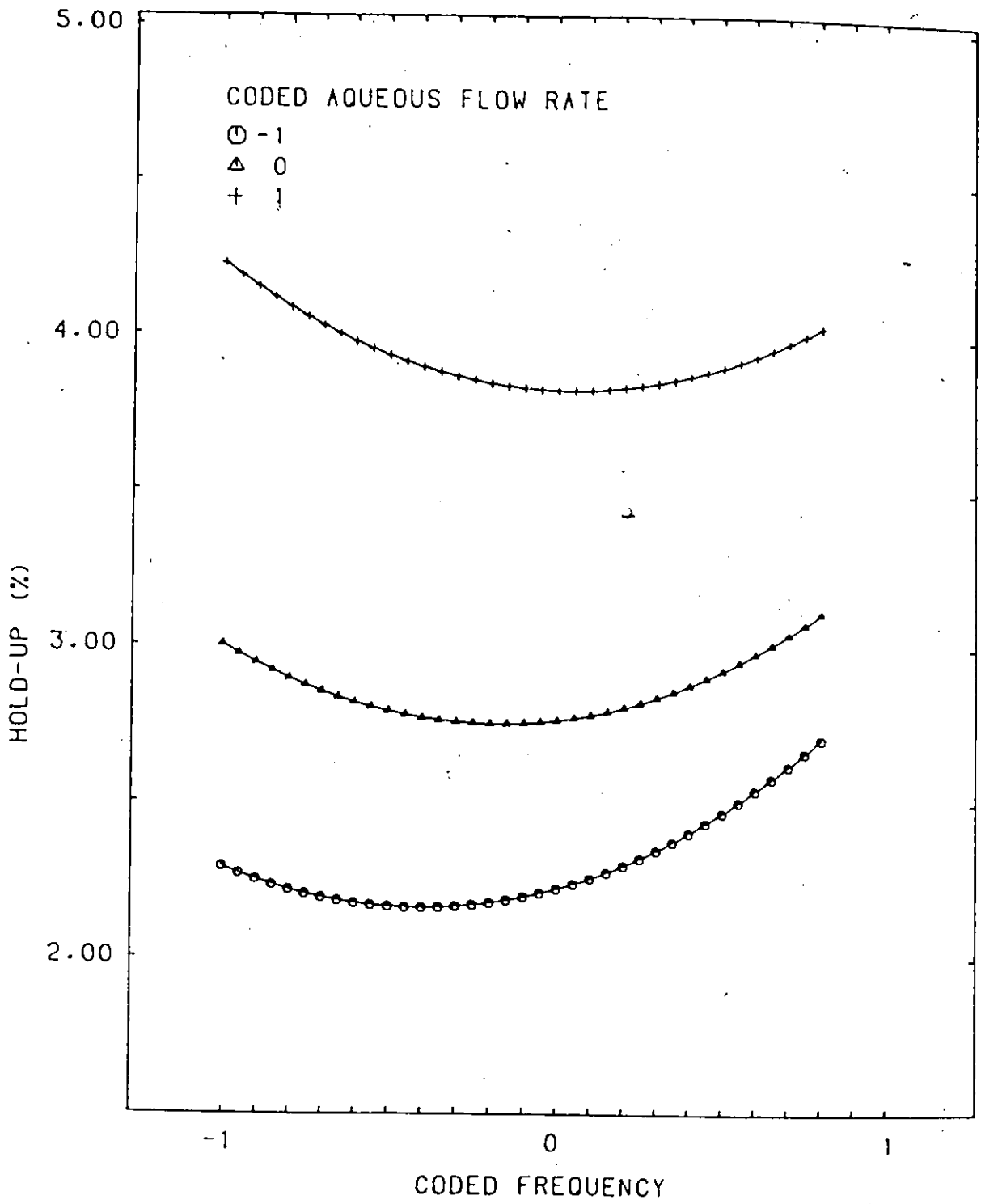

FIGURE 18: PREDICTED HOLD-UP FOR DATA SET IV

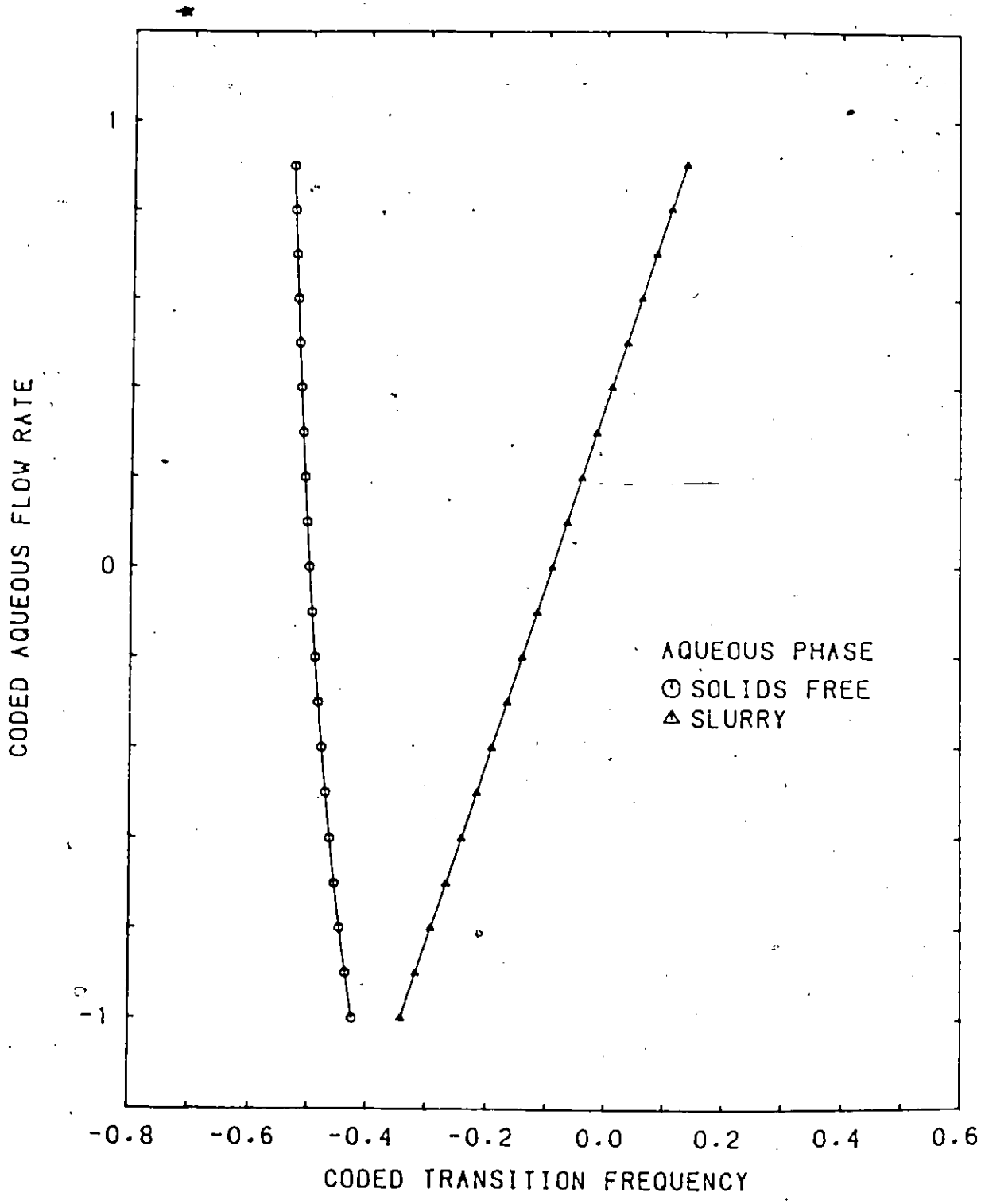

FIGURE 19: PREDICTED TRANSITION FREQUENCY AS A FUNCTION OF AQUEOUS FLOW RATE

6.2.2 DISPERSED PHASE HOLD-UP

Predicted dispersed phase hold-ups for clear aqueous feeds and slurry feeds are compared in Figure 20. The confidence intervals indicate that the hold-up is significantly lower when solids are added to the aqueous phase. As a first attempt at trying to explain this difference, the physical properties of the two aqueous phases were compared (see Table 14). The density and viscosity were found to be higher while the interfacial tension was lower for the slurry. This last estimate is subject to some uncertainty since the amount of solids actually collecting at the interface is not known.

After a drop is formed, it falls from plate to plate at a velocity which determines the hold-up. Using the estimated properties, Equations (27) and (28) predict a higher terminal velocity for the slurry drops. If the slip velocity V_{slip} is equated to the terminal velocity as suggested by Miyauchi and Oya [14] then Equation (2) predicts a decrease in the hold-up. This is in agreement with the observed results.

Parameter values associated with the continuous phase flow rate (see Equation (31)) indicated a small effect on hold-up for DATA SET III. Values obtained from DATA SET IV were all found to be insignificant (see Table 17). This suggests that the continuous phase flow rate effects the hold-up only minimally for the operating conditions considered here.

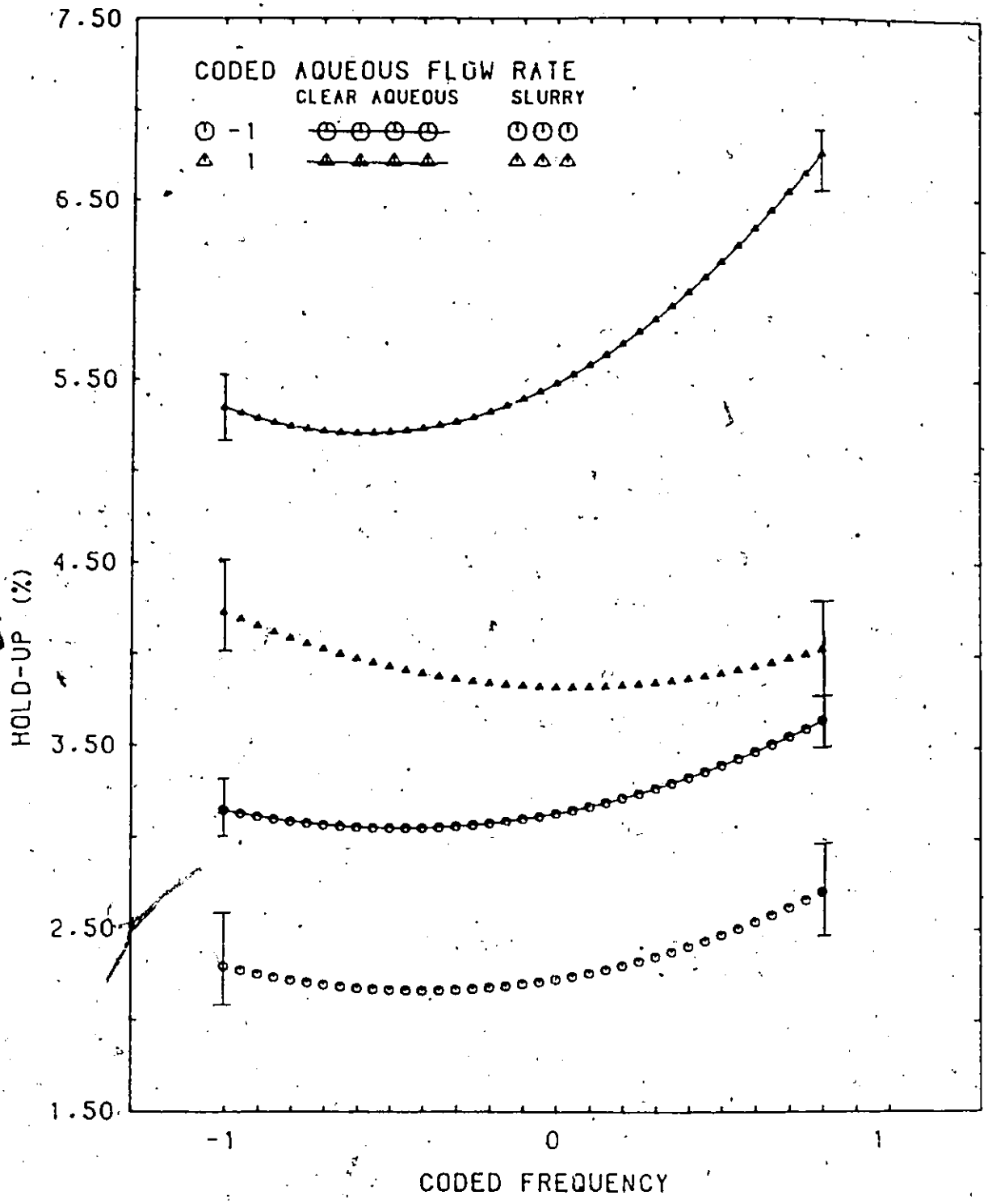

FIGURE 20: PREDICTED HOLD-UP FOR CLEAR AQUEOUS AND SLURRY TESTS

Table 14: PROPERTIES OF CLEAR AQUEOUS AND 10% SLURRY

PROPERTY	CLEAR AQUEOUS	10% SLURRY	
Density (kg/m^3)	1011	1065	Calculated from measured density of solids and pulp
Viscosity $\times 10^3$ (Pa.s)	0.932	1.05	Calculated from Einstein equation using viscosity of the carrier liquid and the concentration and size distribution of solids
Interfacial Tension (mN/m)	10.6	5-7	Measured using ring method by sprinkling sand on interface between two liquids

6.2.3 DROP SIZE

Results from Table 12 show that the presence of solids in the aqueous phase increased drop sizes by 25%. Considering the drop mechanics involved (Equation (26)), differences in physical properties indicate that the slurry phase should form smaller drops. This would suggest that this analysis does not take into account some phenomena unique to drop formation in slurry systems. It is suspected that the effect the solids have at the interface is not fully taken into account by the decrease in interfacial tension measured.

From the previous discussion (see Section 3.2), once a solid is at an interface its contact angle plays a major role in phase stabilization. Measurement of this parameter would be valuable in explaining any phenomenon occurring. Although it was not feasible to measure the contact angle, a simple experiment proposed by Scarlett [28] can provide an estimate of its value. By shaking the two liquids and solid in a test tube an emulsion is formed, the type of emulsion formed provides an indication of the contact angle. Using this system it was found that the solids stabilized an oil emulsion more readily than an aqueous emulsion. Although water emulsions were formed, they coalesced after only a short period of time. Closer examination also revealed that the solid particles collecting at the oil drop interface protruded more into the water phase. Assuming the solids stabilize an emulsion of the more poorly wetted liquid [27], it can be concluded that the contact angle with the oil phase is less than 90°. For a column producing a dispersion of slurry drops in this oil, certain conclusions can be drawn.

It is expected that drop formation at the plates might be affected. The situation thought to exist while a drop is forming on a plate is shown in Figure 21 for a clear aqueous and a solids containing solution. When sand is present, the interface that is being formed would tend to distort to increase contact area between the solid and the aqueous

phase. This occurs because the sand is more water-wetted than oil wetted. In the drop formation process, this would introduce an extra force that must be overcome before the slurry breaks off and forms a drop. This increased force would be provided by the increased buoyancy force of a larger drop. The presence of sand should then increase D_{32} by increasing the size of the drop formed at the plate. This would be one reason for the larger Sauter Mean Diameter measured for the slurry experiments.

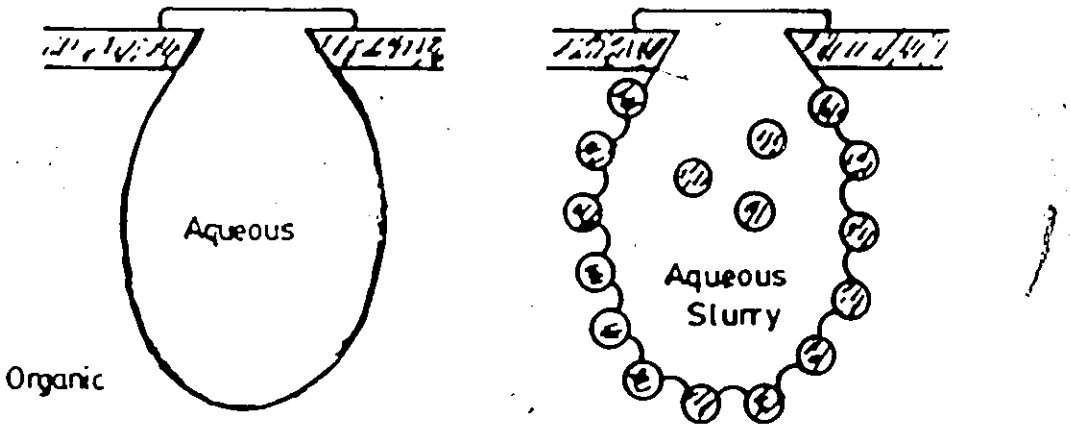

FIGURE 21: DROP FORMATION AT A PLATE

Another effect would occur after the slurry drops were formed in the column. As the presence of solids makes them unstable, the drops would coalesce to produce larger drops having a smaller total surface area. In this way, contact between the solids and the oil is minimized. The photograph in Figure 22 shows that this does occur in the column, any slurry drops that collide after they are formed tend to join and eventually form larger drops. It is suspected that this phenomenon would be more prevalent at high aqueous flow rates since the probabilty of drop contact is higher. The increased drop terminal velocity of the larger drops (see Equation (27) or (28)) would then make emulsion operation more difficult to attain.

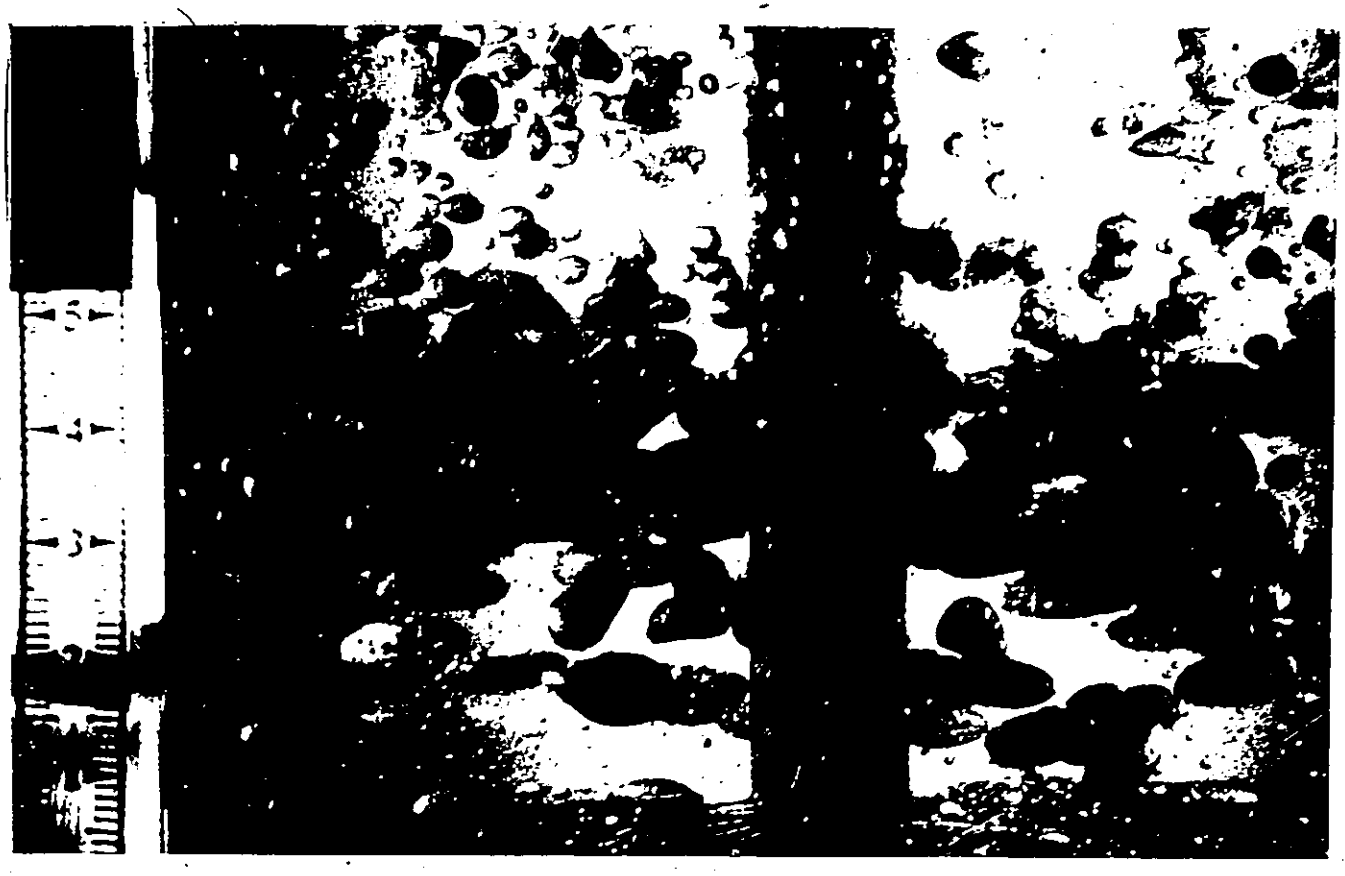

FIGURE 22 SLURRY EMULSION IN COLUMN. Slurry (aqueous + solids) drops falling in the continuous organic phase. Scale shown in cm.

6.2.4 COMPARISON OF HOLD-UP WITH LITERATURE CORRELATIONS

Hold-up values obtained experimentally and those obtained from literature correlations are plotted in Figure 23 and 24. From Figure 23, it is evident that correlations provided by Sato et al [39] and Arthayukti [40] underestimate hold-ups, in some cases by as much as 55 percent. Predictions from the correlation provided by Miyauchi and Oya [14] gave better results. For DATA SET IV, approximate system properties from Table 14 were used to calculate predictions (see Figure 24). Miyauchi and Oya's correlation overpredicts the hold-up by as much as 93 percent for this system. Predictions from Sato et al's are within 50 percent of the observations while those obtained with Arthayukti's are within 30 percent. For both systems, the classifications provided by the correlations indicate operation in the dispersion region. The correlation provided by Kumar and Hartland [15] (see Equations 11-14) was found to underpredict all values of hold-up by 50 percent. This model places the data points in the mixer-settler and dispersion regions.

An empirical correlation containing four constants was proposed by Bell and Babb to predict hold-up over the entire operating region (see Equation 15). This correlation was inadequate for DATA SETS I and II as it provided poor estimates and parameters whose confidence intervals included zero. For DATA SETS III and IV the predictions were better,

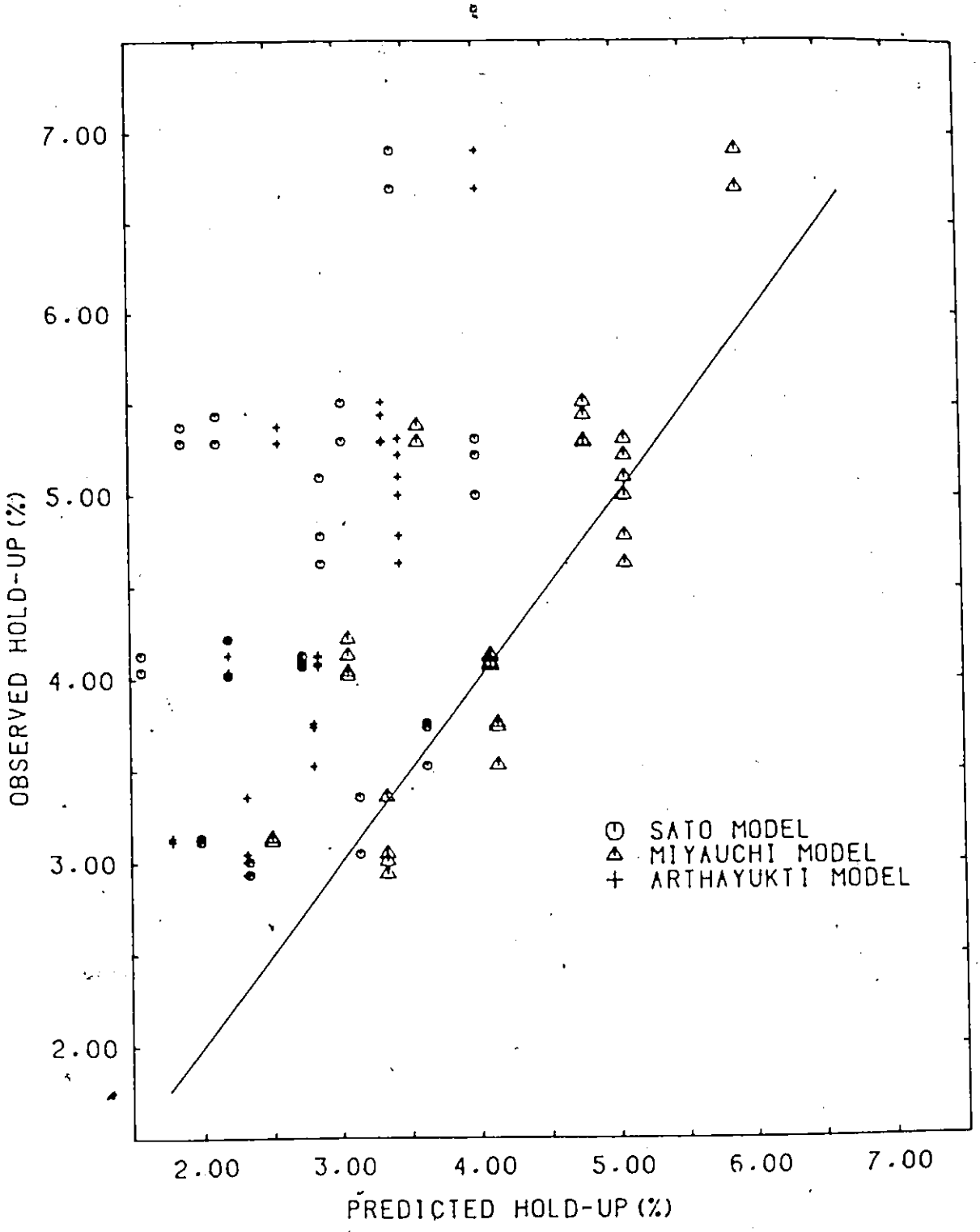

FIGURE 23: PREDICTED HOLD-UP FROM THE LITERATURE FOR DATA SET III

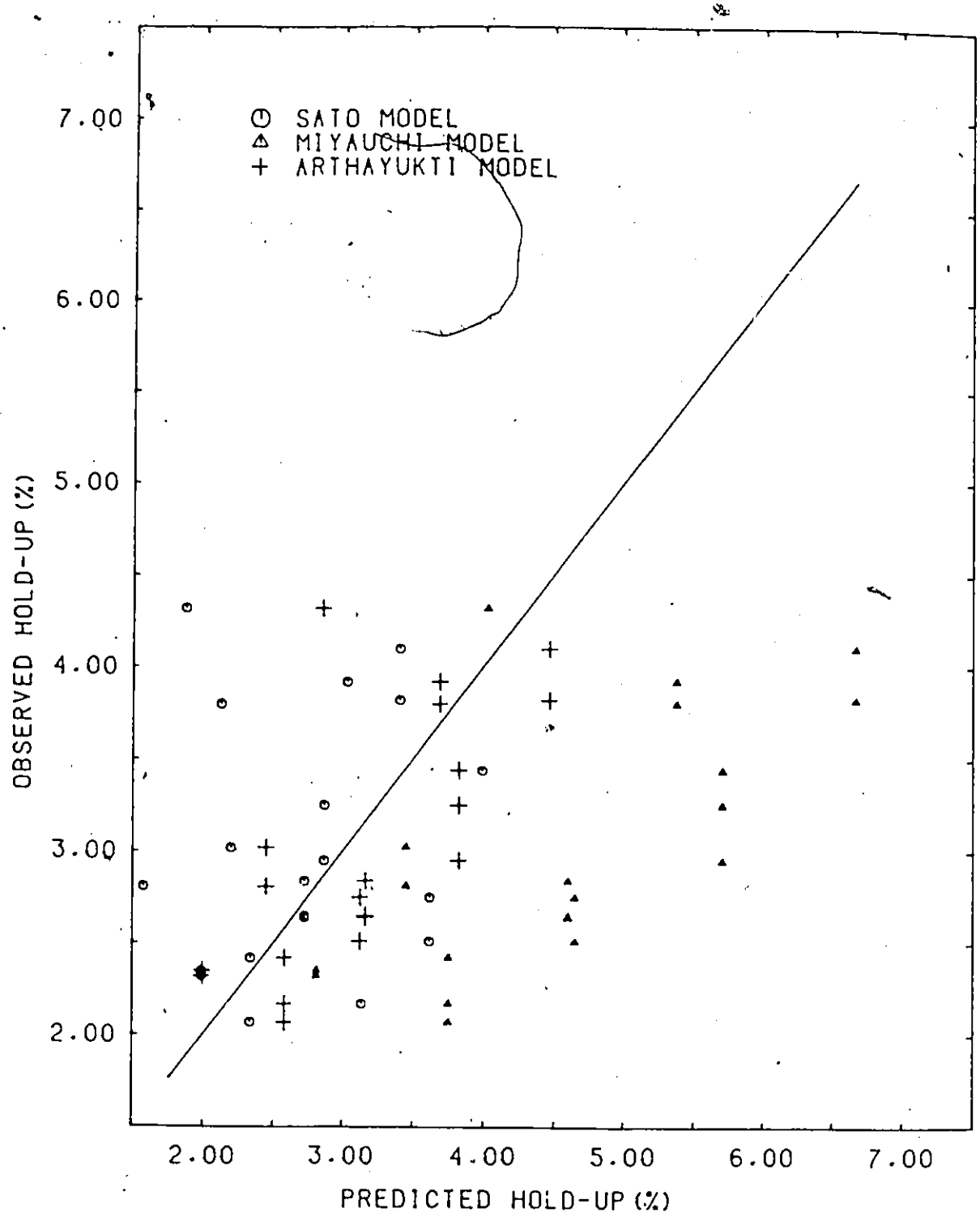

FIGURE 24: PREDICTED HOLD-UP FROM THE LITERATURE FOR DATA SET IV

the parameter estimates for DATA SET III were:

$$C_1 = 3.11\times10^{-3} \pm 4.79\times10^{-2}$$
$$C_2 = 3.31\times10^{-7} \pm 2.11\times10^{-7}$$
$$C_3 = 4.38\times10^{-8} \pm 2.75\times10^{-8}$$
$$C_4 = 6.70\times10^{1} \pm 3.02\times10^{0}$$

For DATA SET IV, the following estimates were obtained:

$$C_1 = 2.22\times10^{-3} \pm 9.62\times10^{-5}$$
$$C_2 = -1.58\times10^{-7} \pm 6.40\times10^{-7}$$
$$C_3 = 7.95\times10^{-8} \pm 8.71\times10^{-8}$$
$$C_4 = 7.65\times10^{1} \pm 4.49\times10^{0}$$

(values of cm/min were used for F×A, V_d and V_c). Since the continuous phase flow rate did not significantly affect the hold-up of DATA SET IV, intervals for C_2 and C_3 include zero. The intervals for these parameters though do include values predicted for DATA SET III which would indicate that they (C_2 and C_3) depend on column geometry as proposed by Bell and Babb [16]. Although this type of model fits the data, correlation between the parameters provided high variances. In the future, it is recommended that specific experiments be planned to lower these correlations in order to obtain better estimates of the parameters.

6.3 SOLVENT LOSSES

Since it has been shown for this system that the solids used stabilize an organic emulsion more readily than an aqueous one, losses are expected to be smaller if the continuous phase is the organic rather than the aqueous phase. In areas where there is a large collection of aqueous phase, some organic might be occluded producing an emulsion. An emulsion formed in this way would be stable and represent a solvent loss since the drop's larger density would force it towards the aqueous phase outlet. This phenomenon was observed to a large extent at the controlled interface at the bottom of the column. In this area, the large volumes of aqueous phase present surrounded and stabilized small volumes of the organic phase. The sequence of events thought to be occurring are shown in Figure 25.

If this same system were maintained as aqueous continuous it is expected that stable emulsions would be formed resulting in high solvent losses. For this case, as soon as the organic drops were formed, the solids in the aqueous phase would migrate to the drop surface. This would stabilize them and make subsequent coalescence virtually impossible. The increased weight of these particles would cause many to flow towards the aqueous outlet. The losses would be directly proportional to the hold-up and the concentration of solids in the aqueous phase.

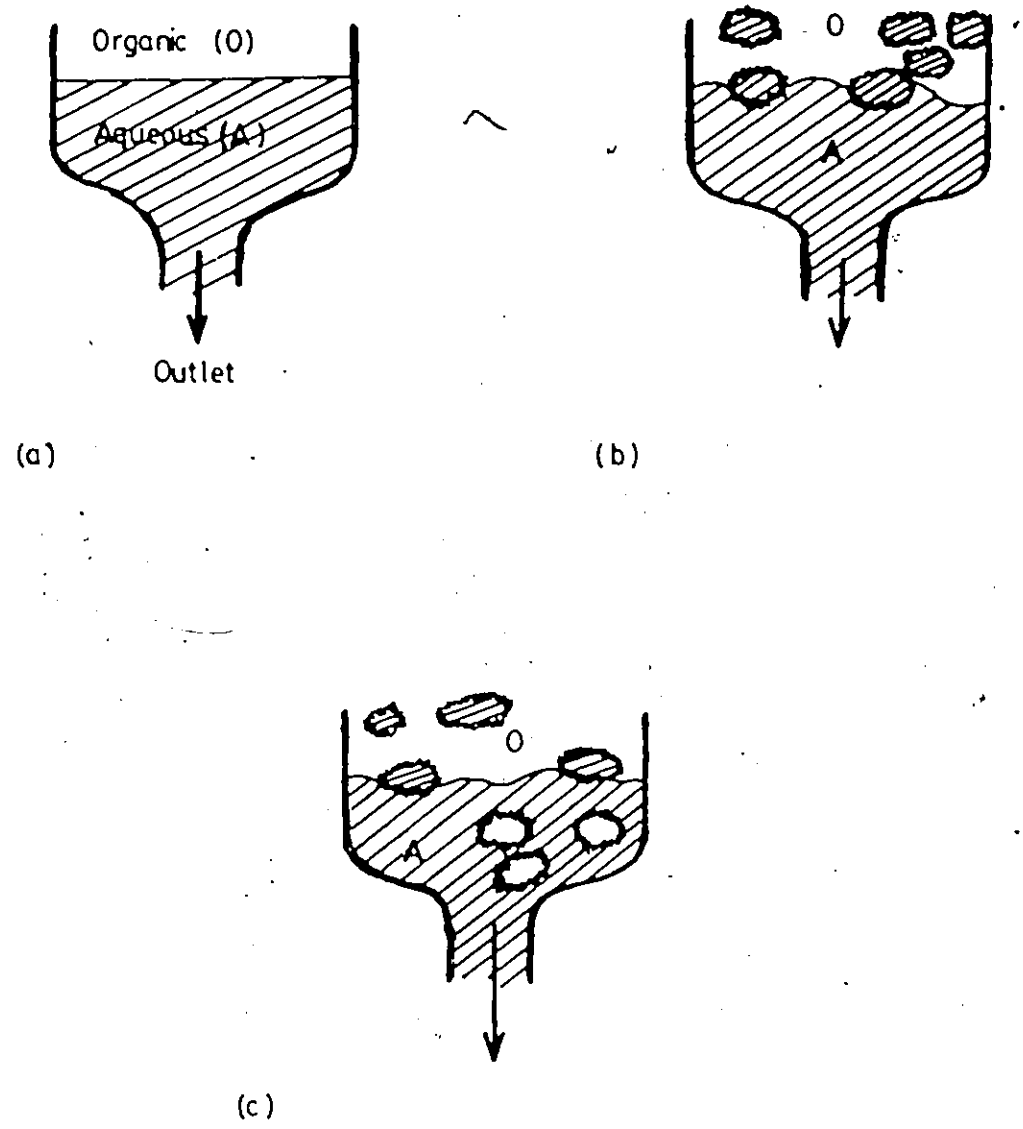

FIGURE 25: SOLVENT LOSSES AT INTERFACE

6.4 EFFECT OF PARTICLE SIZE

This set of tests was performed in an attempt to collect data with a solids size similiar to that which might be encountered in industry [3,5]. A comparison of the hold-up data for the two size distributions studied is presented in Figure 26. The points shown are average values of duplicate tests, 95% confidence intervals are also provided. Apparent from the Figure is the large experimental deviation obtained for the experiments involving the 'Fine Sand'. Due to this, it is possible that the true values of the hold-up for both particle sizes were the same. The larger deviation was thought to have occurred because of the increased solvent entrainment observed with the finer solids, this being caused by the larger total surface area available with the smaller particles. Since the aqueous phase was continually recycled, it would contain increasing amounts of the organic phase. To avoid this problem and to obtain reliable results with systems experiencing large solvent losses, it is recommended that the aqueous phase not be recycled. Another alternative is to install solvent separation equipment to treat the aqueous phase before it is recycled.

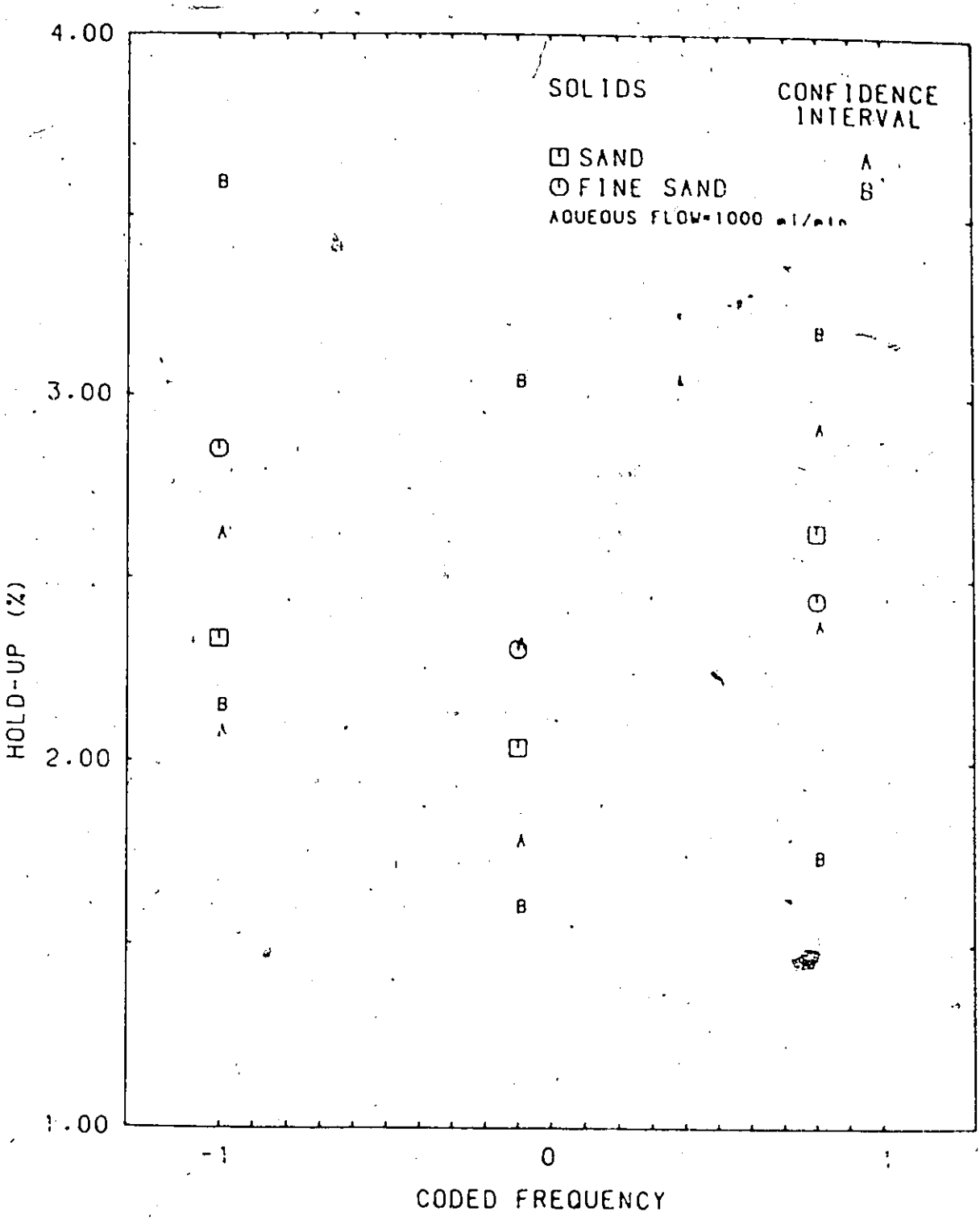

FIGURE 26: AVERAGE DATA COLLECTED FOR DIFFERENT PARTICLE SIZES

6.5 EFFECT OF pH

To study the changes in the surface properties of the solids, tests were performed with an aqueous phase of a different pH. For oxide materials such as quartz (SiO_2) the surface acquires a charge by ionization in water. When quartz or silica is crushed under water, the broken bonds at the surface react with water molecules to form a surface silicic acid [37]. The ionization of this acid creates a charge on the surface of the quartz as follows:

$$Si(OH)_4 \rightleftharpoons Si(OH)_3^- + H^+$$

If the pH is between 1 and 4 the acid would be for the most part undissociated leaving a zero charge on the surface. In this instance the solids tend to agglomerate [22] and become hydrophobic, the zero surface charge making the solids more attracted to a non-polar liquid like oil. This would account for the presence of solids at the interface observed at this pH level. If the pH is raised above 4 the equilibrium shifts to the right and a negative charge is created on the particles. When this occurs, the solids become hydrophilic (i.e. they are attracted to water since it is a polar liquid) and tend to disperse in the aqueous phase. In this case, the solids would become less attracted to the interface, which would reduce their stabilizing effect. Reduction in drop sizes and solvent losses should be observed. However, its effect on the hold-up can not be predicted.

Hold-up data collected at a low pH (1.7) and a high pH (5.5) are shown in Figure 27. Considering the confidence intervals shown, a pH change did not significantly change the hold-up. Further insight into this phenomenon could be obtained if the drop sizes of these two sets of data were compared. Due to equipment failure this was not possible.

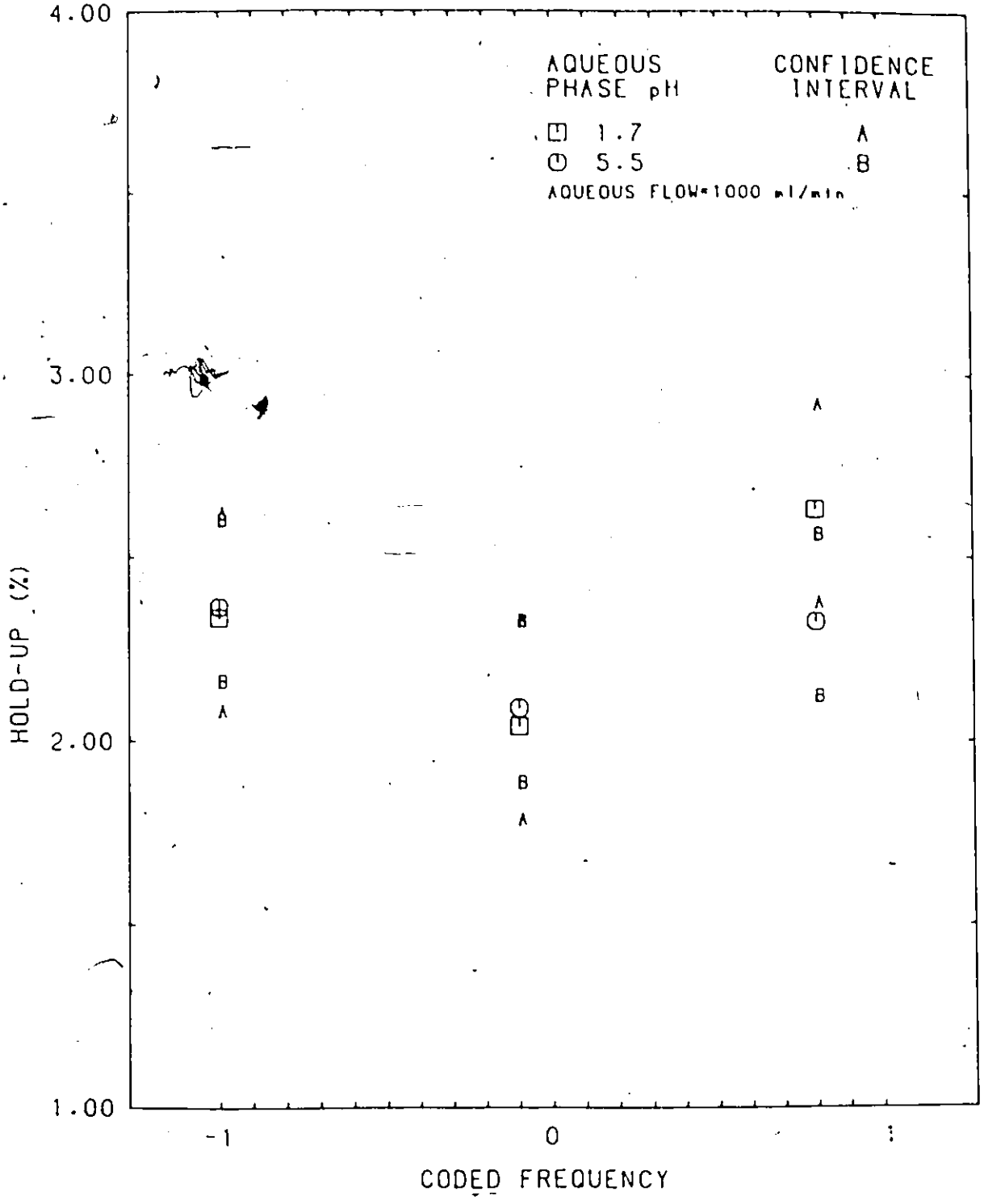

FIGURE 27: AVERAGE DATA COLLECTED FOR DIFFERENT AQUEOUS pH VALUES

Chapter VII

CONCLUSION

A pulsed column was successfully set up to test the hydrodynamics of solvent-in-pulp processing. The addition of solids produced erosion problems on the slurry pump which could be reduced by better selection of equipment.

The presence of solids in the aqueous feed of such a column changed the apparent operating regime as compared to results with clear solutions. In addition, lower dispersed phase hold-ups and larger drop sizes were measured. Smaller hold-ups were accounted for by changes in the physical properties of the slurry. Increases in drop sizes were explained by considering the surface properties of the solids. These surface properties indicate lower solvent losses if the organic phase is maintained as the continuous phase.

The results suggest that the surface properties of the solids influence the hydrodynamics as well as solvent losses in a pulsed column. If this process is to be better utilized, it is recommended that studies examining these relationships be carried out. In this way procedures can be determined by which organic phase wetting can be minimized.

Appendix A

STATISTICAL CONSIDERATIONS

The fractional factorial design used was first proposed by Box and Behnken [41]. For three operating variables the tests included are shown in the Table 15. For each factorial design the experiments described must be carried out and a response value measured. The following variables were calculated and included in the least squares analysis:

$$X_1 \quad X_2 \quad X_3 \quad X_1^2 \quad X_2^2 \quad X_3^2 \quad X_1X_2 \quad X_1X_3 \quad X_2X_3 \quad X_1^2X_2 \quad X_1X_2^2$$

A computer program then estimated values of the parameters associated with each of these variables.

A 95% confidence interval was then estimated for each of the parameters calculated. This describes an interval which has a 0.95 probability of containing the true value of the parameter. It is generally expressed as:

$$\hat{B}_i \pm t_{\nu,0.025}(\text{estimated variance of } \hat{B}_i)^{1/2} \qquad \text{(A1)}$$

Table 15: CODED VALUES OF VARIABLES IN FRACTIONAL FACTORIAL DESIGN

X_1	X_2	X_3
+1	+1	0
+1	-1	0
-1	+1	0
-1	-1	0
+1	0	+1
+1	0	-1
-1	0	+1
-1	0	-1
0	+1	+1
0	+1	-1
0	-1	+1
0	-1	-1
0	0	0
0	0	0
0	0	0

Here $\hat{B}_i$ is the least squares estimate of B_i and $t_{\nu,0.025}$ is the upper 2.5% value of the t distribution and ν is the number of degrees of freedom associated with the pure error variance s^2 The estimated variance of $\hat{B}_i$ is obtained by multiplying the diagonal elements of the $(X^TX)^{-1}$ matrix outputed by the computer by the estimate of the pure error variance. For one set of m replicates s^2 is obtained using the expression:

$$s^2 = \Sigma(y_u-\bar{y})^2/(m-1) \qquad (A2)$$

where $\bar{y}$ is the sample mean response and m is the number of data points. These values can be pooled to obtain a superi-

or estimate from l sets of replicates at different operating conditions using the relationship below:

$$s_p^2 = \Sigma(m_i-1)s_i^2/\Sigma(m_i-1) \qquad (A3)$$

where m_i is the number of data points in the i^{th} set of replicates. Pooling can only be carried out if all the estimates of s^2 are estimates of a common variance s_p^2. Using Bartlett's test [38] this assumption can be tested. For the experiments carried out Bartlett's test confirmed that the individual estimates of the pure error variance from the first three DATA SETS were estimates of a common variance. The results for these sets were thus pooled to obtain s_p^2. For DATA SET IV s_p^2 was obtained only from replicates performed with solids. Once the confidence intervals were calculated those parameters whose intervals included zero were dropped from the model.

An analysis was then performed with the remaining parameters to obtain a new model. The residuals from this new model were plotted versus each operating variable (i.e. X_1, X_2 and X_3). Any deficiencies with respect to these variables were then compensated for by inserting a term into the model. For example, in DATA SET I residuals increased with values of the operating variable X_1. To take this into account the X_1 term was added to the model even though it was found to be insignificant in the earlier analysis.

Once the final changes were made model adequacy was tested by comparing the ratio

$$T = \frac{\Sigma e_u^2/(n-p)}{s_p^2} \qquad (A4)$$

with the value of $F_{(n-p,\nu)}$ at the desired probability level. If the ratio calculated is smaller than the test statistic any inadequacy in the model is not significantly larger than the experimental error and the model is accepted.

Appendix B

FLOW RATE CALIBRATIONS

B.1 AQUEOUS FLOW RATE

It was observed early in this study that the output from the aqueous pump varied over time. To ensure a steady flow rate, a flow measuring device was added to the aqueous feed line. An orifice meter was decided upon because of its simple design and its ability to handle low solids concentrations.

Preliminary calculations to determine the size of the orifice were carried out using the design equation below [42]:

$$Q = \frac{C_D A_O}{(1-C_D^2 A_O^2/A_1^2)^{0.5}} (2g\Delta h)^{0.5} \qquad (A5)$$

To obtain the orifice area A_O values for Q (flow rate), A_1 (pipe cross sectional area) and Δh (difference in manometer height) were needed (C_D was assumed to be 0.62). The Equation was solved iteratively to obtain A_O. The Reynold's number was then calculated to check the initial guess of C_D. This procedure was repeated until the value assumed for C_D was confirmed by the Reynold's number calculation. These calculations provided a good estimate of the orifice hole diameter.

Dimensions of the orifice meter used are given in Figure 28. The pressure taps shown (see Figure) are connected by tygon tubing to small reservoir containers which protect the manometer fluid from contamination, Meriam No. 3 fluid of specific gravity 2.95 was used.

The calibration procedure consisted of measuring the volume delivered per unit time as a function of the difference in manometer heights (Δh). An equation of the form:

$$Q = C_1(\Delta h)^{C_2} \tag{A6}$$

was fit to the data. For the solids free experiments the following equation was obtained:

$$Q = 653.6(\Delta h)^{0.51} \tag{A7}$$

for Q (ml/min) and Δh (inches).

Slurry flow was calibrated using an aqueous solution with a solids concentration of approximately 10% by weight. For this case the calibration equation obtained was:

$$Q = 695.9(\Delta h)^{0.57} \tag{A8}$$

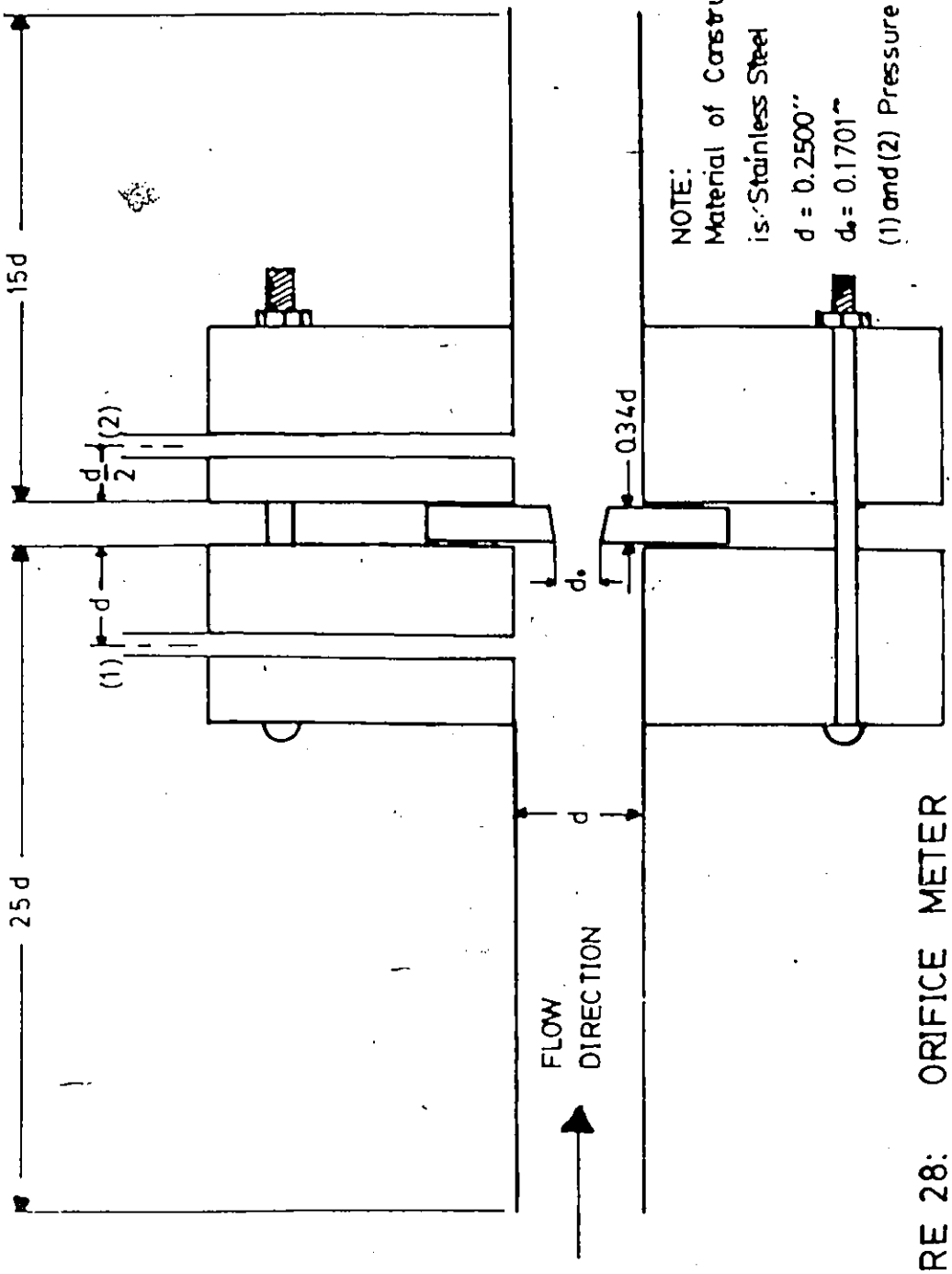

FIGURE 28: ORIFICE METER

B.2 ORGANIC FLOW RATE

Calibration consisted of measuring the volume of organic delivered for a specified time period at each of the operating levels. Results of these tests are presented in Table 16. Other measurements performed during this study indicate flow rate variations of approximately 3%.

Table 16: CALIBRATION DATA FOR ORGANIC PUMP

%CAPACITY	VOLUME COLLECTED (ml)	TIME (s)	FLOW RATE (ml/min)	CODED VALUE
2.0	405	63.65	381.8	-0.99
2.0	409	65.15	376.7	-1.01
4.75	410	42.40	580.2	0.01
4.75	420	43.60	578.0	-0.01
7.5	417	32.10	779.4	1.00
7.5	415	32.00	778.1	1.00

Appendix C

ZEISS PARTICLE SIZE ANALYSER

This equipment is designed for data acquisition and computation of geometric characteristics. The basic units are: digitizer-tablet, computer and monitor.

Co-ordinate data is generated at the tablet whenever a structure is outlined with the stylus. The data is rapidly and continuously calculated into preselected geometric parameters by the dedicated computer. An integrated dual floppy disk drive is utilized for program and data storage.

The most important part of the system is the digitizer-tablet. It functions due to the presence of a magnetic field provided by ferro-magnetic wires spaced at regular intervals in X and Y directions. The wires conduct electronically induced magnetic pulses which are emitted at a constant frequency and travel at a constant speed in both directions. The stylus, when positioned or moved on the surface of the tablet intercepts these X and Y pulses continuously. Co-ordinate data are then derived from these interceptions.

Before beginning an analysis, the desired parameters are indicated to the computer. In this analysis, those chosen were:

1. AREA -area enclosed by the structure
2. DELL AB -major (A) and minor (B) axes of an ellipitical type structure
3. FORM ELL -form factor calculated as B/A
4. DCIRCLE -diameter of a circle of equivalent area
5. VSPHERE -volume of a circular type structure based on DCIRCLE

A scale factor must also be indicated when structures have been enlarged photographically. Once these were chosen, the program is started and structures outlined. After completion of each outline the values of various geometric parameters are displayed on the monitor. When the measurements are completed the data is stored so that it may be analysed.

To obtain an estimate of the Sauter Mean Diameter (D_{32}) the data were transformed using the program PARAMETER ARITHMETIK. Maximum and minimum diameters measured for each droplet were used in this program to obtain equivalent diameters. These were then summed up as described previously to obtain D_{32}.

Appendix D

ADDITIONAL STATISTICAL RESULTS

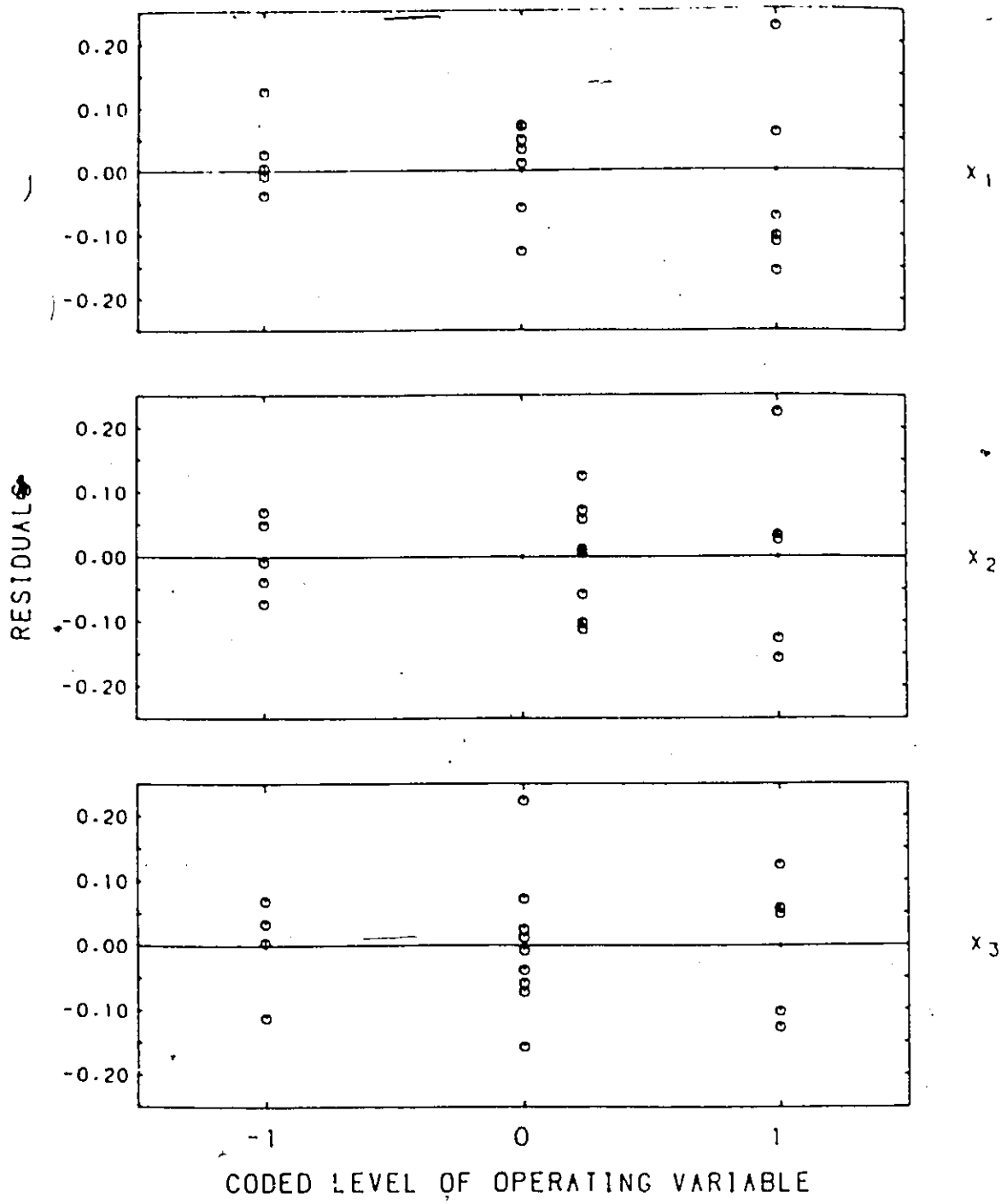

FIGURE 29: RESIDUALS VERSUS OPERATING VARIABLES FOR DATA SET 1

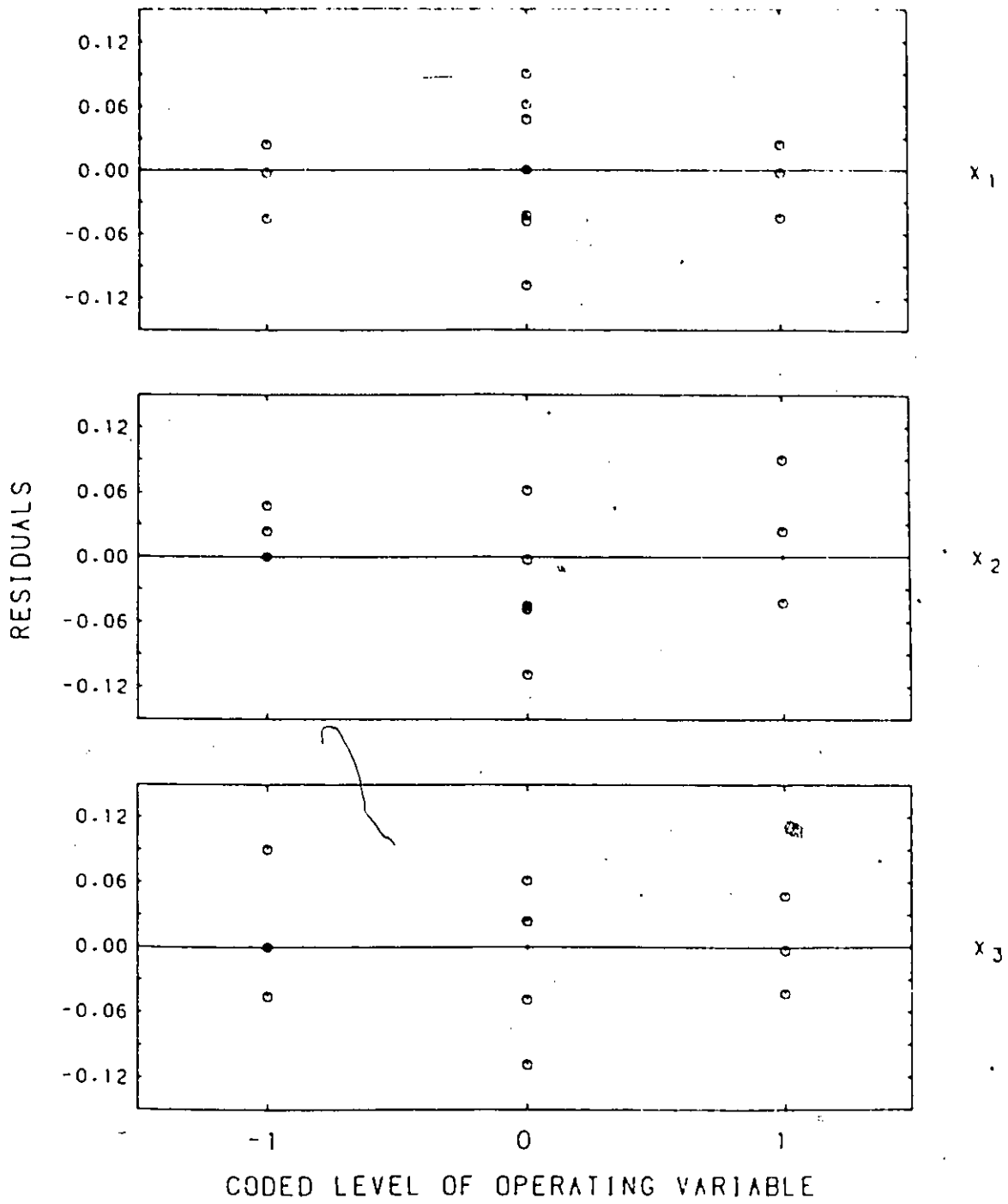

FIGURE 30: RESIDUALS VERSUS OPERATING VARIABLES FOR DATA SET II

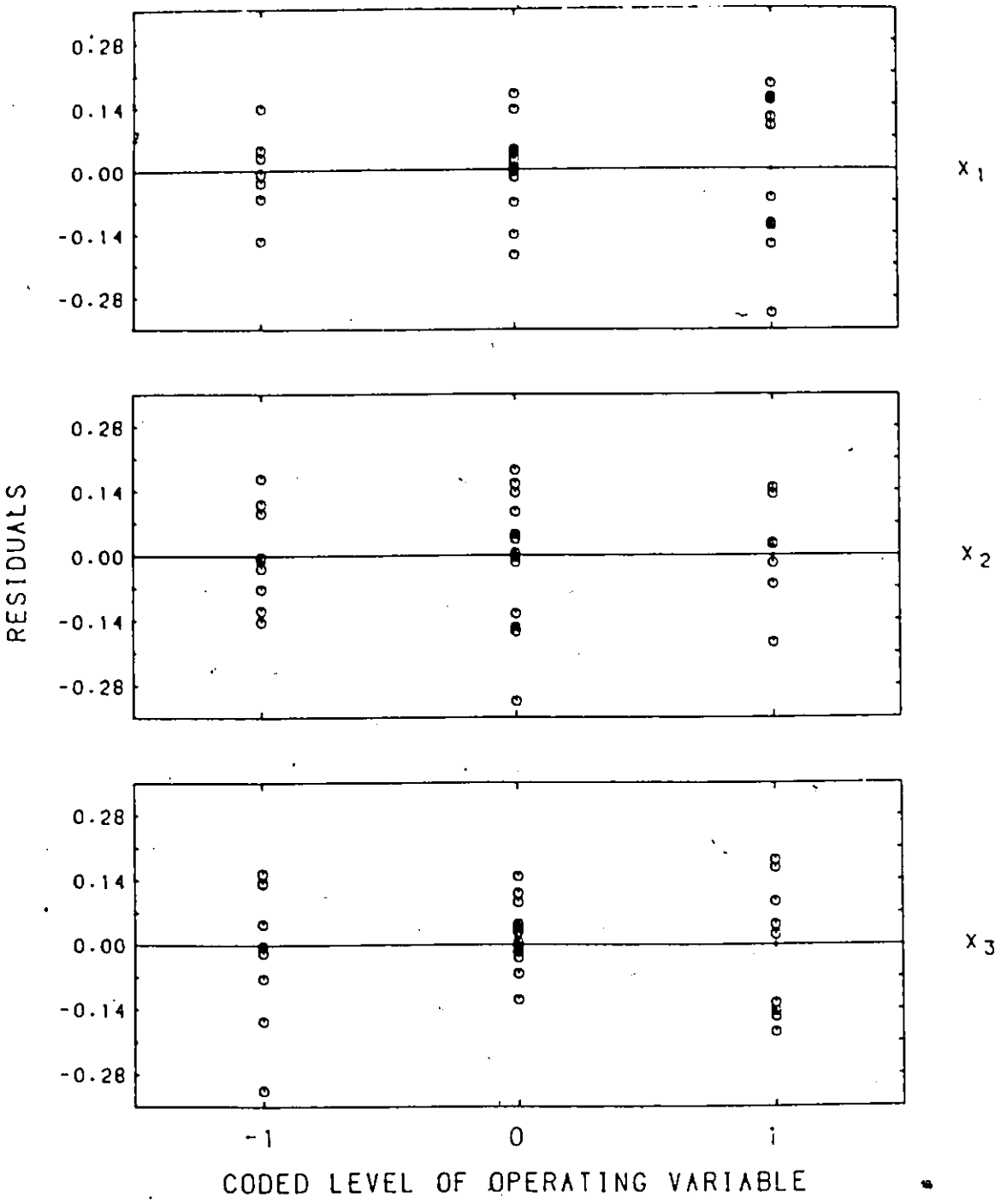

FIGURE 31: RESIDUALS VERSUS OPERATING VARIABLES FOR DATA SET III

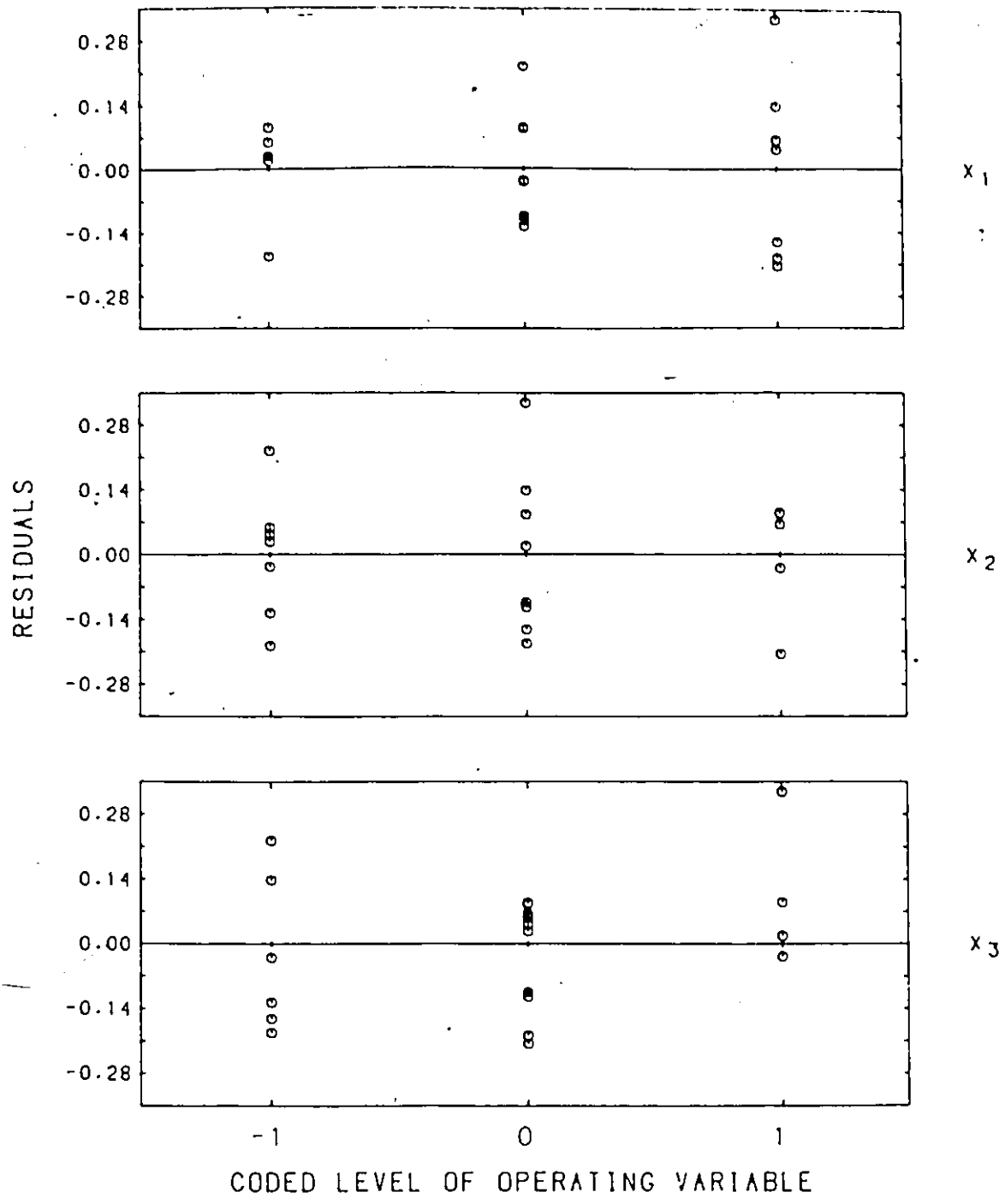

FIGURE 32: RESIDUALS VERSUS OPERATING VARIABLES FOR DATA SET IV

Table 17: PARAMETER ESTIMATES AND CONFIDENCE INTERVALS

PARAMETER	ESTIMATED VALUE (CONFIDENCE INTERVAL) DATA SET I	DATA SET II	DATA SET III	DATA SET IV
B_0	2.4094 (0.1304)	4.4485 (0.1265)	4.0849 (0.0880)	2.7536 (0.1757)
B_1	-0.0658 (0.1301)	-1.0575 (0.1317)	0.4751 (0.0615)	0.0548 (0.1148)
B_2	1.3021 (0.0862)	1.6300 (0.1317)	1.1475 (0.0931)	0.8164 (0.1148)
B_3	0	0.1213 (0.0931)	0.0906 (0.0621)	0
B_4	0	-0.1898 (0.1366)	0.4751 (0.0939)	0.3033 (0.1781)
B_5	-0.3228 (0.1391)	0	0.1651 (0.0926)	0.2595 (0.1781)
B_6	-0.1768 (0.1296)	-0.1473 (0.1366)	0	0
B_7	-0.1624 (0.1128)	-0.1425 (0.1317)	0.2248 (0.0888)	-0.1526 (0.1500)
B_8	0	0	0	0
B_9	0	0	0	0
B_{10}	-0.1299 (0.1753)	-0.2375 (0.1862)	0.1798 (0.1287)	0
B_{11}	0	0.2650 (0.1862)	0	0

BIBLIOGRAPHY

1. Campbell, M.C., G.M. Ritcey and W.A. Gow. C.I.M. Bulletin. 78,139 (1985).
2. Ritcey, G.M., E.G. Joe and A.W. Ashbrook. Transact. A.I.M.E. 238,330 (1967).
3. Ritcey, G.M., M.J. Slater and B.H. Lucas. Proc. Second Intnl. Hydrometallurgy Symposium Chicago. 17,419 (1973).
4. Ritcey, G.M. Chem. Ind. 1294 (1971).
5. Joe, E.G., G.M. Ritcey and A.W. Ashbrook. Journal of Metals. 1,18 (1966).
6. Van Dijk, W.J.D. U.S. Patent. 201,186 (1935).
7. Sege, G. and F.W. Woodfield. Chem. Eng. Prog. 50,396 (1954).
8. Treybal, R.E. "Liquid Extraction". McGraw Hill Inc., New York (1963).
9. Hafez, M.M., M. Nemecek and J. Prochazka. Proceedings of the Int. Solvent Extraction Conf. (ISEC) 1974. 1671 (1974).
10. Sehmel, G.A. and A.L. Babb. Ind. Eng. Chem. Process Design and Development. 2,38 (1963).
11. Batey, W., T. Arthur, P.J. Thompson and J.D. Thornton. Proceedings of the Int. Solvent Extraction Conf. (ISEC) 1983. 166 (1983).

12. Thornton, J.D. Trans. Inst. Chem. Engrs. 35,316 (1957).

13. Niebuhr, O. and A. Vogelpohl. Second World Congress of Chemical Engineers 1981. 2,122 (1981).

14. Miyauchi, T. and H. Oya. A.I.Ch.E.J. 11,295 (1965).

15. Kumar, A. and S. Hartland. Chem. Eng. Res. Des. 61,248 (1983).

16. Bell, R.L. and A.L. Babb. Ind. Eng. Chem. Proc. Des. Dev. 8,392 (1969).

17. Khemangkorn, V., G. Muratet and H. Angelino. Proceedings of the Solvent Extraction Conf. 1,429 (1979).

18. Ellis, D.A., R.S. Long and J.B. Byrne. Second U.N. International Conf. on the Peaceful Uses of Atomic Energy, Geneva. 3,499 (1958).

19. Grinstead, R.R., K.G. Shaw and R.S. Long. Proceedings of the International Conf. on the Peaceful Uses of Atomic Energy, Geneva. 8,1523 (1955).

20. North, A.A. and P.A. Wells. Trans. Inst. Mining and Metallurgy. 74,463 (1964).

21. Burger, J.C. and J.M. Jardine. Second U.N. International Conf. on the Peaceful Uses of Atomic Energy, Geneva. 3,3 (1958).

22. Tolun, R. Second U.N. International Conf. on the Peaceful Uses of Atomic Energy, Geneva. 502,2466 (1958).

23. Wilkinson, W.D. "Uranium Process Metallurgy". Interscience Publishers, New York (1962).

24. Scheele, G.F. and B.J. Meister. A.I.Ch.E.J. 14,9 (1968).

25. Klee, A.J. and R.E. Treybal. A.I.Ch.E.J. 2,444 (1956).

26. Briggs, T.R. J. Ind. Eng. Chem. 13,1008 (1921).

27. Finkle, P., H.D. Draper and J.H. Hildebrand. J. Am. Chem. Soc. 45,2780 (1923).

28. Scarlett, J.A. J. Phys. Chem. 31,1566 (1927).

29. Bacon, D.W. Ind. Eng. Chem. 62,27 (1970).

30. Draper, N.R. and H. Smith. "Applied Regression Analysis". John Wiley and Sons Inc., New York (1966).

31. Jiricny, V. and J. Prochazka. Chem. Eng. Sci. 35,2237 (1980).

32. Kagan, S.Z., M.E. Aerov, V. Lonik and T.S. Volkova. Intnl. Chem. Eng. 5,656 (1965).

33. Cermak, A.F. Proc. Intnl. Solvent Extraction Conf. (ISEC) 1980. 164 (1980).

34. Logsdail, D.H. and J.D. Thornton. Trans. Inst. Chem. Eng. 35,331 (1957).

35. Nanda, A.K. and M.M. Sharma. Chem. Eng. Sci. 21,707 (1966).

36. Fernandes, J.B. Recent Advances in Separation Techniques, A.I.Ch.E. Symposium Series. no.120,68,124 (1968).

37. Aplan, F.F. and D.W. Fuerstenau in D.W. Fuerstenau (ed.). "Froth Flotation". p.170. A.I.M.E. New York (1962).

38. Perry, R.H. and C.H. Chilton (ed.). "The Chemical Engineers' Handbook 6th edition". p.2-100. McGraw Hill Book Company, New York (1984).

39. Sato, T., K. Sugihara and I. Taniyama. Kagaku Kogaku. 27,583 (1963).

40. Arthayukti, W. PhD Thesis Universite Paul-Sabatier, Toulouse. (1975).

41. Box, G.E.P. and D.W. Behnken. Technometrics. 2,455 (1960).

42. Roberson, J.A. and C.T. Crowe. "Engineering Fluid Mechanics". p.533. Houghton Mifflin, Boston (1965).